Received: 8 November 2023 | Accepted: 4 September 2024

DOI: 10.1002/ajb2.16441

RESEARCH ARTICLE

American Journal of Botany

# Eco-phylogenetic study of *Trebouxia* in southern Africa reveals interbiome connectivity and potential endemism in a green algal lichen photobiont

Ian D. Medeiros[1] | Alicia Ibáñez[2] | A. Elizabeth Arnold[3] | Terry A. Hedderson[4] | Jolanta Miadlikowska[1] | Adam Flakus[5] | Ignazio Carbone[6] | Scott LaGreca[1] | Nicolas Magain[7] | Edyta Mazur[5] | Reinaldo Vargas Castillo[8] | József Geml[9] | Maya Kaup[10] | Gillian Maggs-Kölling[11] | Shuzo Oita[3] | Jaya Seelan Sathiya Seelan[12] | Elizaveta Terlova[13] | Erik F. Y. Hom[10] | Louise A. Lewis[13] | François Lutzoni[1]

[1]Department of Biology, Duke University, Durham, NC, USA

[2]Independent Researcher, Gamboa, Panama

[3]School of Plant Sciences, Department of Ecology and Evolutionary Biology, and Bio5 Institute, University of Arizona, Tucson, AZ, USA

[4]Bolus Herbarium, Department of Biological Sciences, University of Cape Town, Cape Town, South Africa

[5]W. Szafer Institute of Botany, Kraków, Poland

[6]Center for Integrated Fungal Research, Department of Entomology and Plant Pathology, North Carolina State University, Raleigh, NC, USA

[7]Biologie de l'évolution et de la Conservation, Université de Liège, Liège, Belgium

[8]Universidad Metropolitana de Ciencias de la Educación, Santiago, Chile

[9]Eötvös Loránd Research Network, Eszterházy Károly Catholic University, Eger, Hungary

[10]Department of Biology, University of Mississippi, University, MS, USA

[11]Gobabeb Namib Research Institute, Gobabeb, Namibia

[12]Institute for Tropical Biology and Conservation (ITBC), Universiti Malaysia Sabah, Kota Kinabalu, Sabah, Malaysia

[13]Department of Ecology and Evolutionary Biology, University of Connecticut, Storrs, CT, USA

**Correspondence**

Ian D. Medeiros, Department of Botany, NMNH MRC 166, Smithsonian Institution, P.O. Box 37012, Washington, DC 20013-7012 USA.
Email: medeirosi@si.edu

**Present addresses**

Ian D. Medeiros, Department of Botany, National Museum of Natural History, Smithsonian Institution, Washington, DC, USA.

Scott LaGreca, Sarah P. Duke Gardens, Duke University, Durham, NC, USA.

Elizaveta Terlova, Cluster of Excellence on Plant Science, Heinrich-Heine-Universität Düsseldorf, Germany.

## Abstract

**Premise:** Southern Africa is a biodiversity hotspot rich in endemic plants and lichen-forming fungi. However, species-level data about lichen photobionts in this region are minimal. We focused on *Trebouxia* (Chlorophyta), the most common lichen photobiont, to understand how southern African species fit into the global biodiversity of this genus and are distributed across biomes and mycobiont partners.

**Methods:** We sequenced *Trebouxia* nuclear ribosomal ITS and *rbcL* of 139 lichen thalli from diverse biomes in South Africa and Namibia. Global *Trebouxia* phylogenies incorporating these new data were inferred with a maximum likelihood approach. *Trebouxia* biodiversity, biogeography, and mycobiont–photobiont associations were assessed in phylogenetic and ecological network frameworks.

**Results:** An estimated 43 putative *Trebouxia* species were found across the region, including seven potentially endemic species. Only five clades represent formally described species: *T. arboricola* s.l. (A13), *T.* cf. *cretacea* (A01), *T. incrustata* (A06), *T. lynniae* (A39), and *T. maresiae* (A46). Potential endemic species were not

significantly associated with the Greater Cape Floristic Region or desert. *Trebouxia* species occurred frequently across multiple biomes. Annual precipitation, but not precipitation seasonality, was significant in explaining variation in *Trebouxia* communities. Consistent with other studies of lichen photobionts, the *Trebouxia*–mycobiont network had an anti-nested structure.

**Conclusions:** Depending on the metric used, ca. 20–30% of global *Trebouxia* biodiversity occurs in southern Africa, including many species yet to be described. With a classification scheme for *Trebouxia* now well established, tree-based approaches are preferable over "barcode gap" methods for delimiting new species.

**KEYWORDS**

desert, fynbos, green algae, Mediterranean biome, microbial biogeography, succulent karoo, symbiosis, systematics, *Trebouxiaceae*, Trebouxiophyceae

Southern Africa, in particular the Greater Cape Floristic Region (GCFR), is a biodiversity hotspot of land plants (Goldblatt, 1978; Maggs et al., 1998; Simmons et al., 1998; Verboom et al., 2009; Schnitzler et al., 2011; Cowling et al., 2017; Clark et al., 2022), with endemic vascular plants making up approximately 68% of ca. 8900 plant species in the fynbos-dominated Cape Floristic Region and approximately 40% of ca. 4850 species in the succulent karoo biome (Hilton-Taylor, 1996; Born et al., 2007). Southern Africa also hosts endemic lichen-forming fungi, particularly but not exclusively in the genus *Xanthoparmelia* (Vain.) Hale (Parmeliaceae) and family Teloschistaceae Zahlbr. (Almborn, 1988, 1989; Hale 1989, 1990; Matzer et al., 1997; Crous et al., 2006; Eichenberger et al., 2007; Leavitt et al., 2018; Medeiros and Lutzoni, 2022). The overall number and proportion of endemic lichens is difficult to quantify because many important genera lack modern taxonomic revisions (Fryday, 2015), but endemism may be as high as 52% for terricolous lichen species in the Knersvlakte area of the succulent karoo (Zedda and Rambold, 2009). The region's most distinctive lichen community occurs in the central Namib Desert, where lichens, almost all of them regional endemics, are the dominant vegetation (Schieferstein and Loris, 1992; Wirth, 2010).

Lichen photobionts in southern Africa may or may not show patterns of distribution, biodiversity, and endemism that parallel their fungal partners or plant relatives. Low endemism would be a reasonable expectation given that a single green algal or cyanobacterial photobiont species can occur in geographically distant but ecologically similar environments (Lutsak et al., 2016; Magain et al., 2018; Garrido-Benavent et al., 2020; Muggia et al., 2020; Rolshausen et al., 2020; Medeiros et al., 2021). Algal lineages initially thought to be geographically restricted are often found across a broader range with expanded sampling (Ryšánek et al., 2015). Even in Antarctica, a region often cited as a rare example of high microbial endemism (De Wever et al., 2009; Pessi et al., 2018; Cox et al., 2019), *Trebouxia* S21 is the sole species considered unique to that continent, while nine other species of *Trebouxia* Puymaly (Trebouxiaceae) have been recorded from both Antarctic and non-Antarctic sites (often northern hemisphere sites; Muggia et al., 2020). Under this "everything is everywhere" scenario (Baas Becking, 1934), we would expect lichen photobiont species in southern Africa to also occur in comparable habitats elsewhere in the world. Such distributions would need to be maintained by ongoing dispersal between continents, e.g., through transportation by wind (Câmara et al., 2023).

On the other hand, surveys of lichen photobionts in previously unstudied regions regularly recover novel putative species (Leavitt et al., 2015; Singh et al., 2017; Muggia et al., 2020; Medeiros et al., 2021; De Carolis et al., 2022; Kosecka et al., 2022). Lichen photobionts vary in their climate and microhabitat niches (Werth and Sork, 2010; Peksa and Škaloud, 2011; Dal Grande et al., 2018; Rolshausen et al., 2018, 2020; Medeiros et al., 2021; Vančurová et al., 2018, 2021; Peksa et al., 2022). Accordingly, the diverse climatic and edaphic conditions in southern Africa, especially in the GCFR (van der Niet and Johnson, 2009), could facilitate high β-diversity and the evolution of locally adapted, endemic species. Moreover, arid conditions across much of southern Africa might contribute to a distinctive regional photobiont pool. Deserts are known to host endemic terrestrial algae (Lewis and Lewis, 2005; Flechtner et al., 2013; Fučíková et al., 2014); for example, some lichenized *Trebouxia* species (e.g., *Trebouxia* A18 and A21) have only been reported from deserts of the western United States (Leavitt et al., 2015; Muggia et al., 2020).

Broad (i.e., genus-level) patterns in the structure of photobiont communities can often be inferred from mycobiont identity alone (Wolseley, 1997; Marini et al., 2011; Koch et al., 2023). However, molecular data are required to identify species of cyanobacterial and unicellular algal photobionts associated with lichen-forming fungi (O'Brien et al., 2013; Škaloud et al., 2015; Malavasi et al., 2016; Magain et al., 2017; Muggia et al., 2020). The paucity of DNA sequence data from southern Africa (Appendix S1), beyond being a problem for algal systematics, presents an impediment to lichen ecology and biogeography in the region. Without sufficient molecular data and a corresponding species-level understanding of lichen photobiont biodiversity, we do not know the extent of endemism in the southern African photobiont biota, the distribution of photobiont species across biomes, or the structure of mycobiont–photobiont interaction networks. All

of these are important for developing a science of lichen biology that treats the photobiont as an equally important object of study to the historically prioritized mycobiont. Network analyses in particular provide a bridge between descriptive studies and an understanding of the evolutionary and ecological mechanisms that shape the lichen symbiosis (Chagnon et al., 2018).

This paper is a first attempt to study the biodiversity, biogeography, and ecological interactions of lichenized *Trebouxia* in South Africa and Namibia. *Trebouxia*—the most common photobiont genus in lichens (Miadlikowska et al., 2006; Muggia et al., 2018; Sanders and Masumoto, 2021)—has been recognized for a century (Puymaly, 1924), but a modern understanding of *Trebouxia* systematics began with the discovery that the genus comprises several major clades (Appendix S2) that vary in their geographical distribution and ecological preferences (Helms, 2003; Nelsen et al., 2021). At a finer taxonomic scale, *Trebouxia* species were historically described based on pyrenoid and chloroplast morphology of cultured isolates (Friedl, 1989). While morphology continues to be an essential part of formal species descriptions (Beck, 2002; Škaloud et al., 2018; Barreno et al., 2022; Garrido-Benavent et al., 2022), known genetic variation exceeds observed morphological variation, and most sequence data are from uncultured specimens, i.e., lichen thalli (Muggia et al., 2020; Bordenave et al., 2022). In response, the *Trebouxia* research community has established a classification scheme in which putative species are delimited based on the internal transcribed spacer (nrITS; Appendix S2) and given provisional names (Leavitt et al., 2015; Muggia et al., 2020).

Using *Trebouxia* nrITS and *rbcL* sequence data from diverse lichen mycobionts and biomes, we first placed southern African *Trebouxia* in a global phylogenetic context, allowing us to document the regional biodiversity of the genus and reassess our understanding of *Trebouxia* systematics worldwide. With complementary species delimitations based on phylogenetic and OTU clustering approaches, we then explored how *Trebouxia* biodiversity is distributed across the biomes of southern Africa and assess the biogeography of putative regional endemics. Finally, we investigated the mycobiont–photobiont interaction network to evaluate specificity and generalism and determine whether interaction patterns known largely from northern hemisphere studies hold true in southern Africa.

## MATERIALS AND METHODS

### Sampling and DNA sequencing

Lichens were collected in June–July 2019 from 14 sites across South Africa and Namibia in the desert, forest, fynbos, grassland, savanna, and succulent karoo biomes (Mucina and Rutherford, 2006). The sampling was focused on obtaining diverse mycobionts from a wide range of habitats (Figures 1, 2; Appendix S3). Recent lichen collections from Borneo (June 2018) and Chile (June 2017) were also included to provide additional data on tropical and southern hemisphere *Trebouxia*. Specimens were stored under standard herbarium conditions before DNA extraction.

For most macrolichens and some saxicolous crustose lichens with thick thalli, DNA was extracted with a phenol–chloroform protocol. Approximately 1 $cm^2$ of healthy lichen thallus was frozen with liquid nitrogen and ground with 1 mm zirconia/silica beads in a bead beater. The powder was mixed with 500 µL of 2% w/v SDS–2% w/v PVP lysis buffer and incubated overnight at room temperature. The DNA was purified with the addition of 500 µL of phenol–chloroform–isoamyl alcohol (25:24:1) and 5 min centrifugation at 13,500 RCF, followed by 250 µL of chloroform–isoamyl alcohol (24:1) and 5 min centrifugation at 18,000 RCF. DNA was precipitated from the supernatant with cold isopropyl alcohol and 2 min centrifugation at 18,000 RCF, followed by 5 min centrifugation in cold 80% v/v ethanol at 18,000 RCF. After air drying, the DNA was resuspended in sterile water and 1/10 dilutions were used for PCR.

For most crustose lichens and some macrolichens, we extracted DNA using a modification of the procedure described by Hughes et al. (2020). A sterile needle was used to excise ca. 1 $mm^2$ of lichen thallus, which was placed in 20 µL of extraction buffer and incubated at room temperature for 10–20 min. For samples with a high concentration of secondary metabolites (i.e., the extraction solution turned yellow or red), we replaced the solution with fresh extraction buffer and repeated the incubation. The samples were then frozen at −20°C for approximately 1 h as previously reported (Medeiros and Lutzoni, 2022), thawed at room temperature, and incubated at 95°C for 10 min. Finally, 20 µL of 3% w/v BSA was added to each sample. Extracts were used for PCR without further dilution.

Two loci, nrITS and *rbcL*, were selected for their established use in *Trebouxia* and availability in reference databases (Appendix S2). *Trebouxia* nrITS (including ITS1, 5.8S, and ITS2) was amplified with primers ITS1T and ITS4T (Kroken and Taylor, 2000). The thermal cycling program consisted of 95°C for 3 min; 35 cycles of 95°C for 40 s, 52°C for 40 s, and 72°C for 150 s; and a final extension at 72°C for 10 min. We also amplified *rbcL* with primers a-ch-rbcL-203-5′-MPN and a-ch-rbcL-991-3′-MPN (Nelsen et al., 2011) and thermal cycling conditions of 95°C for 5 min; 40 cycles of 95°C for 1 min, 50°C for 1 min, and 72°C for 1 min; and a final extension at 72°C for 7 min. For all samples, we attempted to amplify the mycobiont nrITS using primers ITS1F (Gardes and Bruns, 1993) and either ITS4 or LR3 (Vilgalys and Hester, 1990; White et al., 1990) or the mycobiont mtSSU using primers mrSSU1 and mrSSU3R (Zoller et al., 1999). PCR conditions were the same as for photobiont nrITS.

PCR success and amplicon size were verified in a 1% agarose gel. PCR products were cleaned with exonuclease I and shrimp alkaline phosphatase (Thermo Fisher, Waltham, MA, USA), then Sanger-sequenced by Eurofins

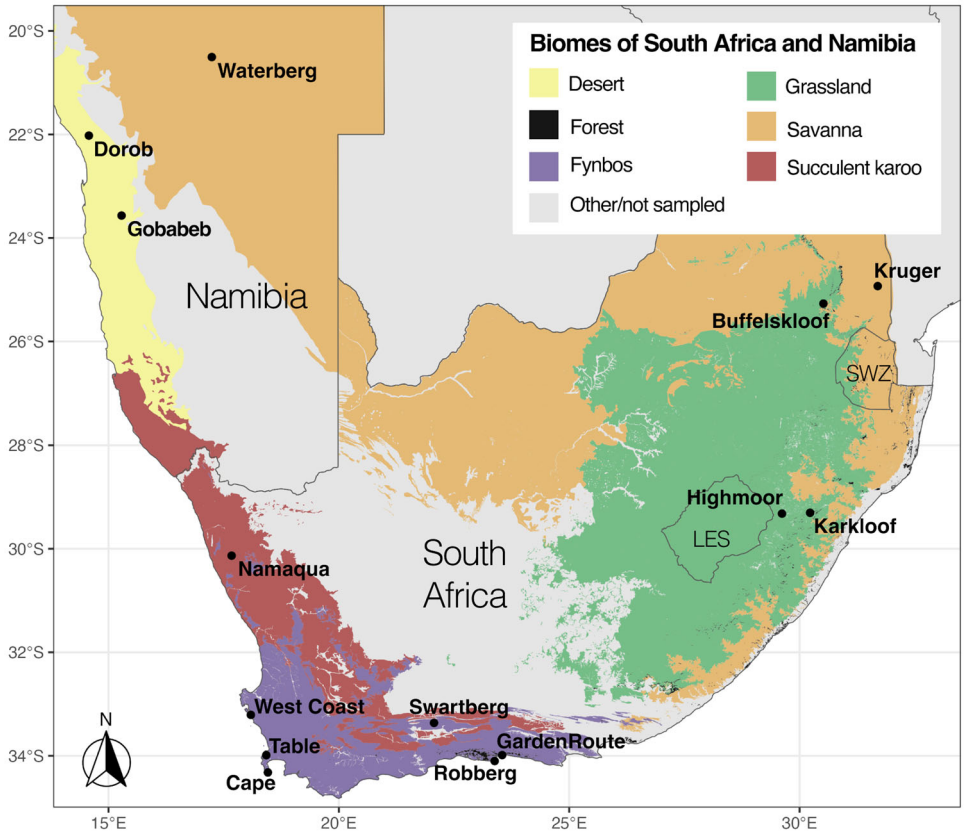


**FIGURE 1** Map of study sites. Biomes sampled in this study are shown on the map; other biomes and areas outside South Africa, Namibia, Lesotho (LES), and Eswatini (SWZ) are in gray. The Greater Cape Floristic Region (GCFR) is approximately equivalent to the extent of the fynbos and succulent karoo biomes.

Genomics (Louisville, KY, USA). Forward and reverse sequences were assembled and trimmed in Geneious Prime (versions 2019.2 through 2023.1 were used during the project; www.geneious.com). Sequences were compared against the NCBI nucleotide database using BLAST (Zhang et al., 2000) to verify that mycobiont molecular and morphological identifications were consistent and that the photobiont nrITS and *rbcL* from a single thallus belonged to the same major clade within *Trebouxia*. GenBank accession numbers for new sequences are included in Appendix S4. A small number of sequences from other genera in Trebouxiophyceae Friedl were obtained during our sampling. These non-*Trebouxia* sequences were not used in subsequent analyses but are provided as additional data on the biodiversity of lichen photobionts in southern Africa (Appendix S5).

## Alignment and phylogeny inference with curated global data set

We assigned new *Trebouxia* sequences to major clades (Appendix S2) with two complementary methods: BLAST against the NCBI nucleotide database and T-BAS with RAxML-EPA (Berger et al., 2011) using a GTR + Γ substitution model and *Trebouxia* reference phylogeny (Carbone et al., 2017, 2019; Medeiros et al., 2021). Once binned into major clades, new sequences were manually added to previously curated, clade-level alignments (Medeiros et al. 2021) in Mesquite 3.70 (Maddison and Maddison, 2021). These alignments were based on the nrITS and *rbcL* reference data sets from Muggia et al. (2020) and Xu et al. (2020). In addition to the data generated in this study, we added South African *Trebouxia* sequences already available in GenBank (Appendix S1) and sequences from putative *Trebouxia* species not included in the Medeiros et al. (2021) data set, i.e., species delimited in overlooked or recent publications (Buckley et al., 2014; Singh et al., 2017; Ruprecht et al., 2020; De Carolis et al., 2022; Kosecka et al., 2022). As done by Medeiros et al. (2021), we excluded putative species A37 and A49 (Muggia et al., 2020) because the single nrITS sequence available for each species was missing a large portion of the ITS2 spacer; preliminary investigation with BLAST indicated that none of our new sequences were closely related to these two putative taxa. For outgroups, we used one specimen from each of the other major clades (Appendix S2), represented by 5.8S and *rbcL*; ITS1 and ITS2 were removed from the outgroup taxa to maximize the number of unambiguously aligned positions. Ambiguously aligned regions were delimited manually and excluded from the phylogenetic analyses. Alignment files are available on Figshare (doi: 10.6084/m9.figshare.c.6661265) and GenBank

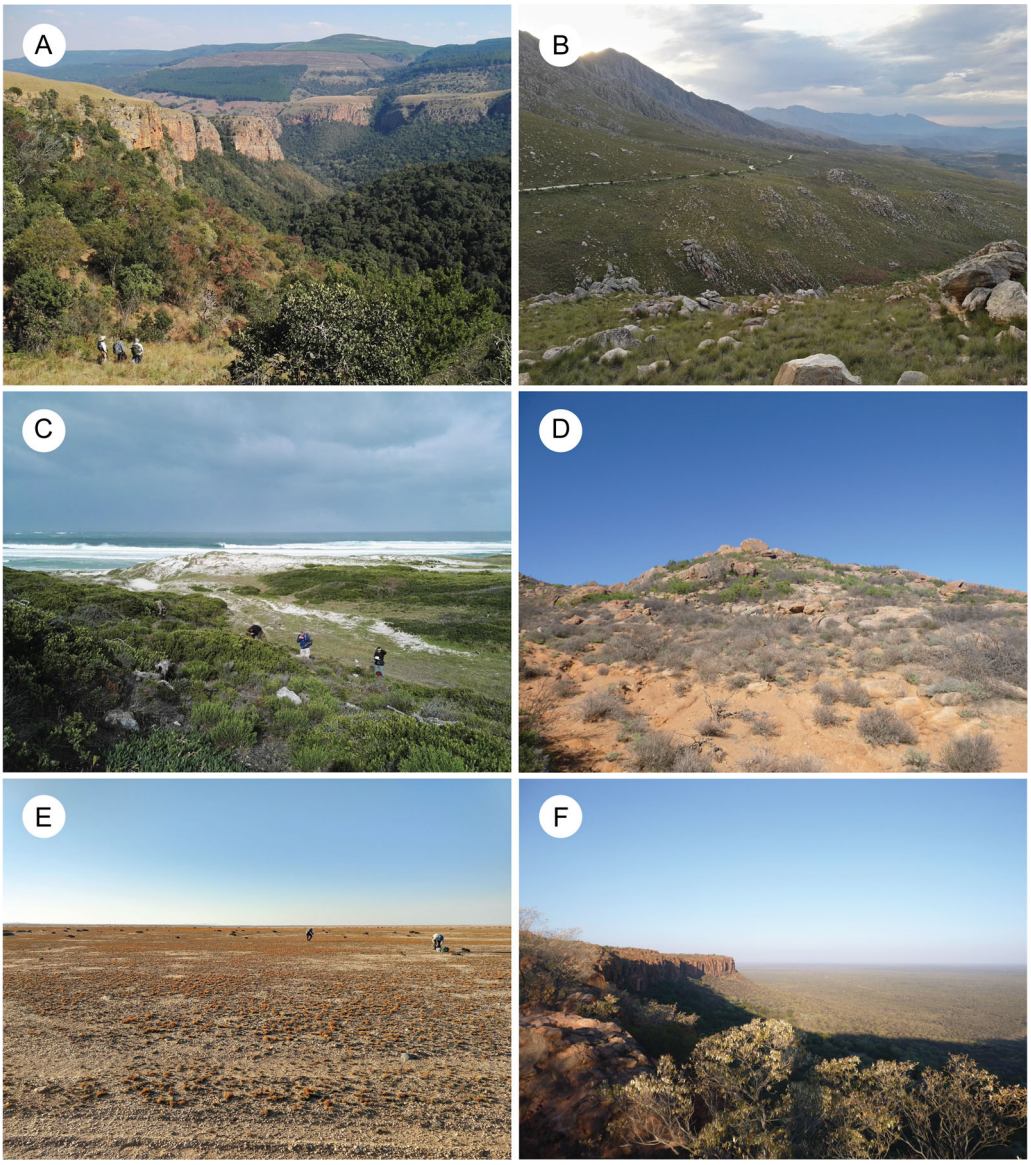


**FIGURE 2** Examples of habitats sampled for lichen photobionts. (A) Northern mistbelt forest in Buffelskloof Nature Reserve, South Africa; (B) fynbos in the Swartberg Nature Reserve, South Africa; (C) fynbos on the Cape peninsula, Table Mountain National Park, South Africa; (D) succulent karoo in Namaqua National Park, South Africa; (E) coastal desert lichen field in Dorob National Park, Namibia; (F) savanna in Waterberg National Park, Namibia. See Appendix S3 for site geographic coordinates. Photographs by Ian Medeiros (A, D, F), József Geml (B, C), and Erik Hom (E).

accession numbers for all samples in the alignments are provided in Appendices S4 and S6. For the remainder of the paper, we refer to these curated, clade-level ITS and *rbcL* alignments as data set A.

Single-locus trees were inferred from data set A via a maximum likelihood analysis in IQ-TREE 2.1.2 (Nguyen et al., 2015; Chernomor et al., 2016) with 1000 ultrafast bootstrap pseudoreplicates used to calculate bipartition support (Hoang et al., 2018). We inspected the resulting trees for well-supported conflicts (≥95% ultrafast bootstrap). Comparison of the single-locus trees for clade A revealed a well-supported conflict between nrITS and *rbcL* for two specimens of *Trebouxia* A29: L1661 and L1739, from Muggia et al. (2014). In both cases, the nrITS sequences (KJ754243 and KJ754246) clustered with other specimens classified as A29, while the *rbcL* sequences (KR914368 and KM091768) clustered with A13. These two samples were removed from subsequent analyses. In the absence of other well-supported conflicts, nrITS and *rbcL* were concatenated. For each clade, we ran a maximum likelihood analysis on the concatenated alignment in IQ-TREE, using the -p and -m MFP + MERGE options to find the optimal partitioning scheme and substitution models (Kalyaanamoorthy et al., 2017). The initial partitioning scheme split the nrITS by region (ITS1, 5.8S, and ITS2) and *rbcL* by codon position; the final partitioning schemes and substitution models are provided in Appendix S7. We used 5000 ultrafast bootstrap pseudoreplicates to calculate bipartition support. Phylogenetic

analyses were run on the CIPRES server (Miller et al., 2010). We also used the single-locus nrITS trees as input for the bPTP web server (Zhang et al., 2013; https://species.h-its.org/ptp/); after preliminary tests, we used the maximum likelihood implementation of PTP because its splitting was substantially more conservative than the Bayesian implementation.

In this paper, we are working within the phylogenetic framework and classification system currently in widespread use for *Trebouxia* (Leavitt et al., 2015; Muggia et al., 2020), although we will also discuss some of its limitations. In this system, nrITS-delimited species receive an alphanumeric code consisting of the clade letter and a two-digit species number. The species recognized in this scheme by Muggia et al. (2020) and subsequent authors (Medeiros et al., 2021; De Carolis et al., 2022; Kosecka et al., 2022) are the starting point for our classification. First, new *Trebouxia* sequences were assigned, when possible, to previously delimited species using a criterion of monophyly (the "monophyly-known species" approach): Samples falling in a well-supported clade (ultrafast bootstrap ≥95%) with reference sequences from a single recognized species were assigned to that species. When the identification was ambiguous (e.g., because of low support), we recorded the closest species with a "cf." designation. Well-supported clades (ultrafast bootstrap ≥95%) lacking reference sequences or singletons with less than 95% BLAST similarity to any other putative species were considered putative novel species.

## Operational taxonomic unit (OTU) clustering with all available nrITS sequences

We assembled a global data set of *Trebouxia* nrITS sequences (data set B) as an alternative to the more curated data set A using the approach of Nelsen et al. (2021) to obtain and filter data. First, we queried the NCBI nucleotide database with the search "internal transcribed spacer OR 5.8S AND *Trebouxia* [ORGN] AND Chlorophyta[ORGN]" on 1 February 2023, which yielded 9061 sequences. These sequences were split into ITS1, 5.8S, and ITS2 with ITSx (Bengtsson-Palme et al., 2013) to identify chimeric, incomplete, misclassified, and non-nrITS sequences, which were excluded after verification with BLAST. For the remaining sequences, ITS1, 5.8S, and ITS2 were concatenated. We used BLAST to identify *Asterochloris* sequences misclassified as *Trebouxia*, using FN556033 as the search query. Finally, we used mothur (Schloss et al., 2009) to remove sequences shorter than 525 bases or with more than three ambiguous bases. Sequences that passed this filtering were placed in the phylogeny of *Trebouxia* in T-BAS, as described above, to bin sequences into major clades and identify long branches that might represent non-*Trebouxia* or low-quality sequences that escaped the initial filtering.

For each major clade, the GenBank data and newly obtained nrITS sequences were merged into a single data set and aligned in MAFFT with either the G-INS-1 (clades A, C, and I) or FFT-NS-I (clade S) strategies (Katoh et al., 2019). Alignments were corrected in Mesquite and the delimitation of ambiguous regions was imported from data set A. At this stage, additional non-*Trebouxia* or suspected low-quality sequences were removed; a complete list of excluded sequences and justifications for their removal is provided in Appendix S8. With the 8092 sequences that passed this quality screening, we adopted an OTU clustering approach using similarity thresholds common in ecological studies (Botnen et al., 2018). After removing the 5′ and 3′ excluded regions, the unaligned nrITS sequences of data set B were clustered at 95% and 97% similarity using VSEARCH (Rognes et al., 2016).

## Evaluating the "barcode gap" in *Trebouxia*

Most species recognized in the current classification framework for *Trebouxia* were delimited with a so-called "barcode gap" method that looks for a discontinuity between intra- and interspecific genetic distances in nrITS sequences (Puillandre et al., 2012, Muggia et al., 2020). While this method has yielded an extremely useful and widely adopted scheme for classifying *Trebouxia* biodiversity, the central assumption of this approach—that a barcode gap exists in *Trebouxia*—has not been evaluated. The presence of a gap might suggest that this approach remains useful for classifying the growing amount of *Trebouxia* sequence data. Conversely, the absence of a gap should cause us to look for alternative methods for delimiting species. If there is no gap, we should also treat species identifications made under the existing framework with caution and consider multiple delimitation approaches when addressing ecological questions.

Data set B was used to calculate two complementary measures of pairwise sequence similarity. First, the nrITS alignments with ambiguously aligned regions removed were used as input for IQ-TREE using the -p and -m MFP options, with the data set partitioned into ITS1 + ITS2 and 5.8S. Distance matrices were calculated from the resulting trees in the R package ape 5.7-1 (Paradis and Schliep, 2019) using the cophenetic.phylo function. In addition to plotting histograms of pairwise distances, we used the distance matrices as input to the ASAP server (https://bioinfo.mnhn.fr/abi/public/asap/asapweb.html; Puillandre et al., 2021) with default parameters to get a measure of total *Trebouxia* species diversity under a "barcode gap" criterion. Second, the 5′ and 3′ excluded regions were removed from the aligned sequences, retaining all internal ambiguous regions. Within each clade, we then performed an all-versus-all comparison of the unaligned sequences with dc-megablast (Zhang et al., 2000). The simMatrix function from the R package RFLPtools 2.0 (Flessa et al., 2022) was used to generate a similarity matrix from the BLAST output, and pairwise similarities were plotted as histograms.

## Recognition of *Trebouxia* species

We obtained a consensus classification for each sample by combining the species identifications from the monophyly-known species approach (data set A), 95% and 97% OTU

clustering (data set B), and PTP analysis (data set A). The results of these methods were compared with the R package networkD3 0.4 (Allaire et al., 2017). When all methods agreed on a species-level group in the southern African data, we adopted the name from the monophyly-known species approach. We did the same when the monophyly-known species, 97% OTU clustering, and PTP delimitations agreed, and the only conflict was with 95% OTU clustering, because 95% is a conservative clustering threshold that would require us to lump well-supported, previously recognized species. For the remainder, we selected the most conservative (i.e., lumping) delimitation among the monophyly-known species, 97% OTU clustering, and PTP criteria. Trees annotated with these consensus species identifications were prepared in R 4.3.1 (R Core Team, 2023) with packages ggtree 3.8.2 (Yu et al., 2017) and ggtreeExtra 1.10.0 (Xu et al., 2021).

## Identification of mycobionts

Lichen mycobionts were identified with primary and secondary taxonomic literature, including keys for southern Africa and biogeographically related regions (Swinscow and Krog, 1988; Almborn, 1989; Stevens, 1999; Kärnefelt et al., 2002; Moberg, 2004; Wirth, 2010; Sipman, 2017). Thin-layer chromatography was performed using standard methods with solvents A, B′, and C (Culberson and Kristinsson, 1970; Culberson, 1972; Culberson and Johnson, 1982). When available, nrITS and mtSSU sequences (Appendix S4) were compared against the NCBI nucleotide database using BLAST. Sequenced voucher specimens are at DUKE or KRAM, with duplicates at ARIZ, BOL, PRE, or WIND.

## Species richness, global comparisons, and endemism

To assess whether we have sufficient data to estimate total *Trebouxia* species richness in the study region, we used the specaccum function from the R package vegan 2.6-4 (Oksanen et al., 2022) to calculate accumulation curves for the entire genus and for each major clade. This analysis and the other biogeographical and ecological analyses that follow were performed with both the consensus species and 97% OTU clusters to ensure that our conclusions are robust to alternative delimitations of *Trebouxia* species.

We compared the southern African *Trebouxia* biota with two other well-sampled areas of the southern hemisphere: Bolivia and Kenya, the best-sampled countries in South America and Africa, respectively. Published species identifications for *Trebouxia* sequences from those countries (Leavitt et al., 2015; Lutsak et al., 2016; Singh et al., 2017; Muggia et al., 2014, 2020; Medeiros et al., 2021; Kosecka et al., 2022) were verified by placement on clade-level phylogenies in T-BAS as described above, and the three regions were also compared in the 97% OTU clustering results (data set B). For each clade, we also used the nrITS trees from data set B to quantify the proportion of global phylogenetic diversity present in southern Africa, Kenya, and Bolivia. Phylogenetic diversity was measured by summing branch lengths with the R package ape.

Southern Africa's endemic plants and lichen-forming fungi are concentrated in the Greater Cape Floristic Region and desert, respectively, the latter defined as <250 mm precipitation per year (Meigs, 1953). To evaluate whether there is an association between novel, potentially endemic *Trebouxia* species and these regions (which overlap in the succulent karoo biome), we calculated the proportion of lichen thalli from the GCFR which contained potentially endemic *Trebouxia* taxa. We defined endemics as consensus species or 97% OTU clusters that only contained southern African samples. For each delimitation approach, we then generated 1000 sets of randomized site–thallus pairs by sampling without replacement to obtain a null distribution of the proportion of GCFR thalli with endemic species, assuming no association between endemism and region. This procedure was repeated for the desert. The percentage of the null distribution greater than or equal to the empirical proportion was taken as the *P*-value, with the significance threshold set at $\alpha = 0.0125$ to account for multiple comparisons.

## Community predictors and interaction networks

Following the approach from Chagnon et al. (2018), we used the function adonis2 in the R package vegan to assess whether, for a given lichen thallus, photobiont identity is better predicted by mycobiont genus, site, or biome. We also used the adonis2 function to quantify the predictive value of mean annual temperature (MAT, BIO1), mean annual precipitation (MAP, BIO12), and precipitation seasonality (BIO15) for explaining variation in *Trebouxia* community composition at the clade, consensus species, and 97% OTU levels. Bioclimatic data were obtained from WorldClim 2 (Fick and Hijmans, 2017) at 2.5-min resolution using the R package terra 1.7.78 (Hijmans, 2024). The community distance matrices were calculated using Bray–Curtis distances and 999 permutations were used for the adonis2 PERMANOVA.

We represented site–photobiont and mycobiont–photobiont associations as networks, which were constructed using the R package igraph 1.3.5 (Csardi and Nepusz, 2006) and visualized with ggraph 2.1.0 (Pedersen, 2022). To assess which sites were most important to the connectedness of the network, we calculated normalized closeness and betweenness centrality with igraph for a subgraph of sites, with edges indicating shared photobiont species, derived from the site–photobiont network. Because there was considerable variation in the number of samples per site (Appendix S3), we generated rarefied/resampled and randomized data sets to compare with the empirical network. For the rarefied/resampled data set, eight thalli (approximately the median number of samples per site) were sampled with replacement from each site. This

procedure was repeated 1000 times to generate a simulated distribution under uniform sampling effort. For the randomized data set (null distribution), we followed the approach used in the test for regional endemism. For both simulated data sets, we constructed the network for each iteration and calculated normalized closeness and betweenness.

For the mycobiont–photobiont network, we grouped mycobionts at the genus rank because most mycobiont species were represented by three or fewer collections and species could not be identified for all samples (Appendix S4). Network modularity was measured and compared to a distribution of scores calculated for a null model (Vázquez et al., 2007) in the R package bipartite 2.1.8 (Dormann et al., 2009) using the procedure from Chagnon et al. (2018), except that we used the modularity algorithm from Beckett (2016). We also measured nestedness of the two bionts with the wNODF index (Almeida-Neto and Ulrich, 2011), using the same null model for comparison and calculating *P*-values as in the test for regional endemism, with $\alpha = 0.05$. We calculated degree and betweenness centrality as complementary metrics for generalism and importance in community structure (González et al., 2010).

# RESULTS

## Phylogeny and species identification

We assembled a data set of *Trebouxia* in South Africa and Namibia from 152 lichen thalli, including new data for 139 specimens and sequences from 13 specimens from previous studies (Nyati et al., 2013, 2014; Singh et al., 2017; Fryday et al., 2020; Moya et al., 2021; Appendix S4). New sequences from Borneo and Chile (13 and eight thalli, respectively) contributed to the phylogenetic data set (Appendix S6). Three South African samples from the literature lacked geographic coordinates and were omitted from biogeographical and ecological analyses. All samples were represented by nrITS and approximately 50% by *rbcL*. Southern African samples were distributed across *Trebouxia* clades A ($N = 58$), C ($N = 59$), I ($N = 30$), and S ($N = 5$), with no samples from clade D. The most common mycobiont families sampled from southern Africa were Parmeliaceae ($N = 60$), Teloschistaceae ($N = 29$), Ramalinaceae ($N = 20$), and Physciaceae ($N = 11$), with smaller numbers from several other families including Acarosporaceae, Candelariaceae, Chrysotrichaceae, Graphidaceae, and Umbilicariaceae (Appendix S4). This represents a broad phylogenetic sampling of *Trebouxia*-associated lichenized fungi spanning three fungal classes (Lecanoromycetes, Lichinomycetes s.l. [including Candelariaceae, Díaz-Escandón et al., 2022], and Arthoniomycetes). Although not the focus of the paper, we note that this study provides the first molecular data for several species of lichen-forming fungi, including *Candelina africana* Poelt., *Heterodermia subcitrina* Moberg, and *Usnea maculata* Stirt.

Preliminary species identifications made with data set A under the monophyly-known species criterion are displayed on clade-level phylogenies in Appendix S9. The OTU clusters obtained from data set B provide an alternative delimitation (Appendix S10). Overall, the number of species recognized by the monophyly-known species criterion was intermediate between the 95% and 97% OTU clustering thresholds, while PTP split species more finely and gave a higher number of putative taxa than any other method (Table 1).

The fate of individual samples under these four approaches is shown in Appendix S11. For 25 of the 43 species delimited under the monophyly-known species criterion, the four methods yielded the same grouping of southern African samples, although they did not always agree on a name. We accepted these species in our consensus classification and, when no named reference sequences were included in a group, gave the clade a new alphanumeric code under the nomenclatural scheme from Muggia et al. (2020). In a further seven cases, the monophyly-known species, 97% OTU clustering, and PTP delimitations agreed, and the only conflict was with 95% OTU clustering. For the remainder, we selected the most conservative delimitation among the monophyly-known species, 97% OTU clustering, and PTP criteria as the consensus species (Appendix S11).

Our consensus classification for clade A divided southern African samples into 15 putative species (Figure 3). A single sample that fell outside any previously delimited species and had low similarity to available nrITS data (top BLAST hit was 93.1% to *T. cretacea* OM275550, with 99% coverage) was recorded as novel species *Trebouxia* A66. Southern African samples clustered with strong support with the formally named species *T. arboricola* s.l. (A13),

**TABLE 1** Delimiting potential species in southern African *Trebouxia*. The number of putative species varied under different criteria: monophyly-known species, OTU clustering at 95% and 97%, and the maximum likelihood implementation of PTP (PTP-ML). The final column gives the total species numbers from the consensus classification.

| | | OTU clustering | | | |
|---|---|---|---|---|---|
| **Clade** | **Monophyly following Muggia et al. (2020)** | **95%** | **97%** | **PTP-ML** | **Consensus classification** |
| A | 15 | 14 | 21 | 34 | **15** |
| C | 16 | 15 | 20 | 17 | **16** |
| I | 11 | 10 | 16 | 22 | **11** |
| S | 1 | 3 | 1 | 1 | **1** |
| *Trebouxia* (total) | 43 | 42 | 58 | 74 | **43** |

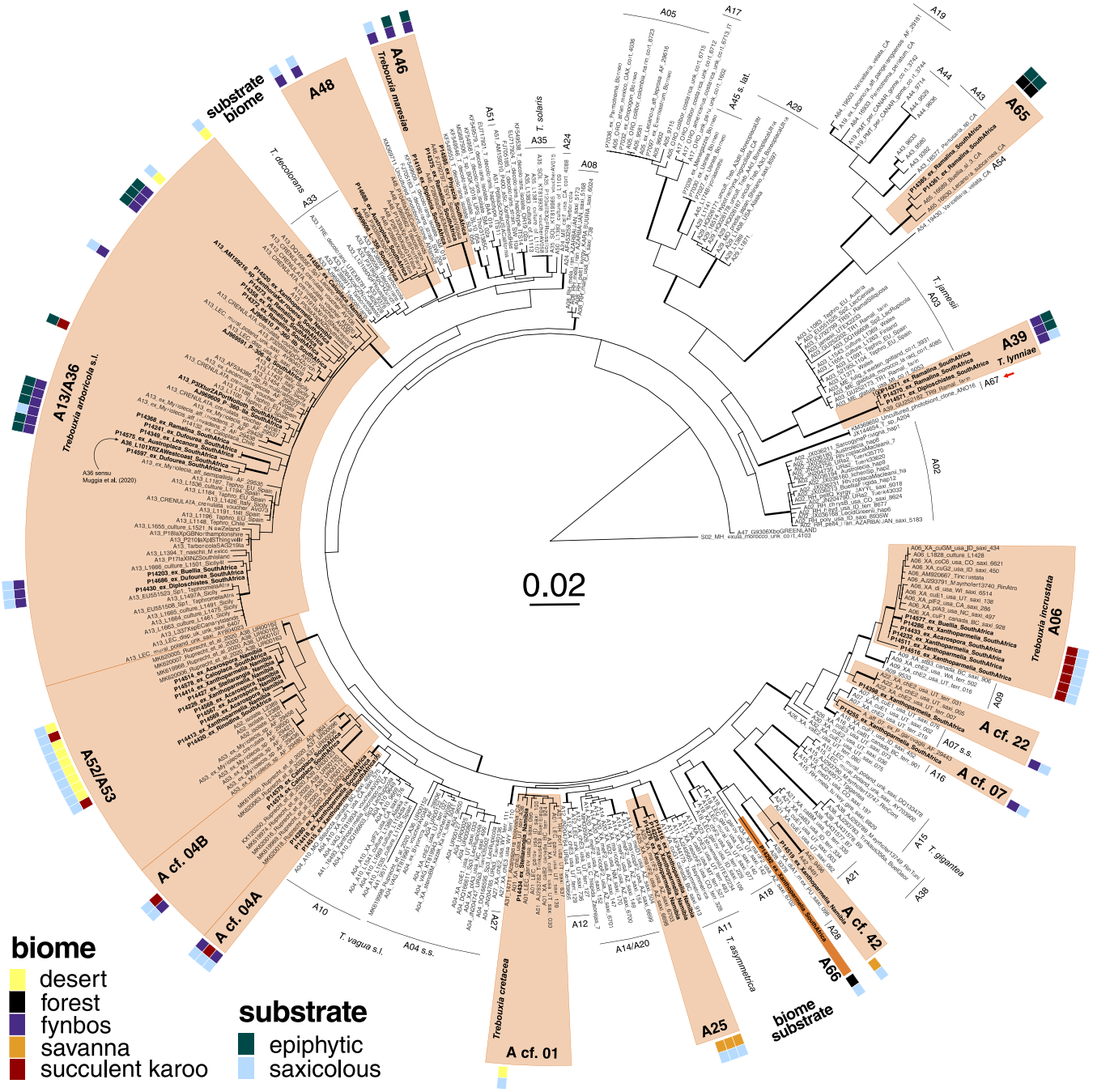


**FIGURE 3** Phylogeny of *Trebouxia* clade A based on maximum likelihood analysis of the concatenated nrITS-*rbcL* (data set A). Thick branches indicate ultrafast bootstrap ≥95%. Samples from southern Africa are indicated with bold text. Putative species-level lineages found in southern Africa are highlighted in orange; pale orange indicates species known from outside the study region; dark orange indicates a novel putative species that is potentially endemic to southern Africa. Biome and substrate are indicated in the inner and outer ring, respectively, for southern African samples. *Trebouxia* A67, indicated with a red arrow, does not occur in southern Africa but is incorporated into the *Trebouxia* classification scheme for the first time. Scale indicates substitutions per site. A version of this tree with all ultrafast bootstrap values ≥ 50% is available in Appendix S9.

*T. incrustata* Ahmadjian ex. Gärtner (A06), *T. lynniae* Barreno (A39; Barreno et al., 2022) and *T. maresiae* Garrido-Benavent, Chiva & Barreno (A46; Garrido-Benavent et al., 2022); one sample also clustered with *T. cretacea* Voytsekhovich & Beck (A01; Muggia et al., 2020), albeit with low support. Apart from our southern African sampling, we found a clade from New Zealand (Buckley et al., 2014; Rafat et al., 2015) that fell outside currently delimited species (Figure 3) and is incorporated into the classification as novel species *Trebouxia* A67.

In the consensus classification for clade C, southern African samples fell into 16 putative species, making this the most speciose major clade in our sampling (Figure 4; Appendix S11). Clade C also had the greatest number of

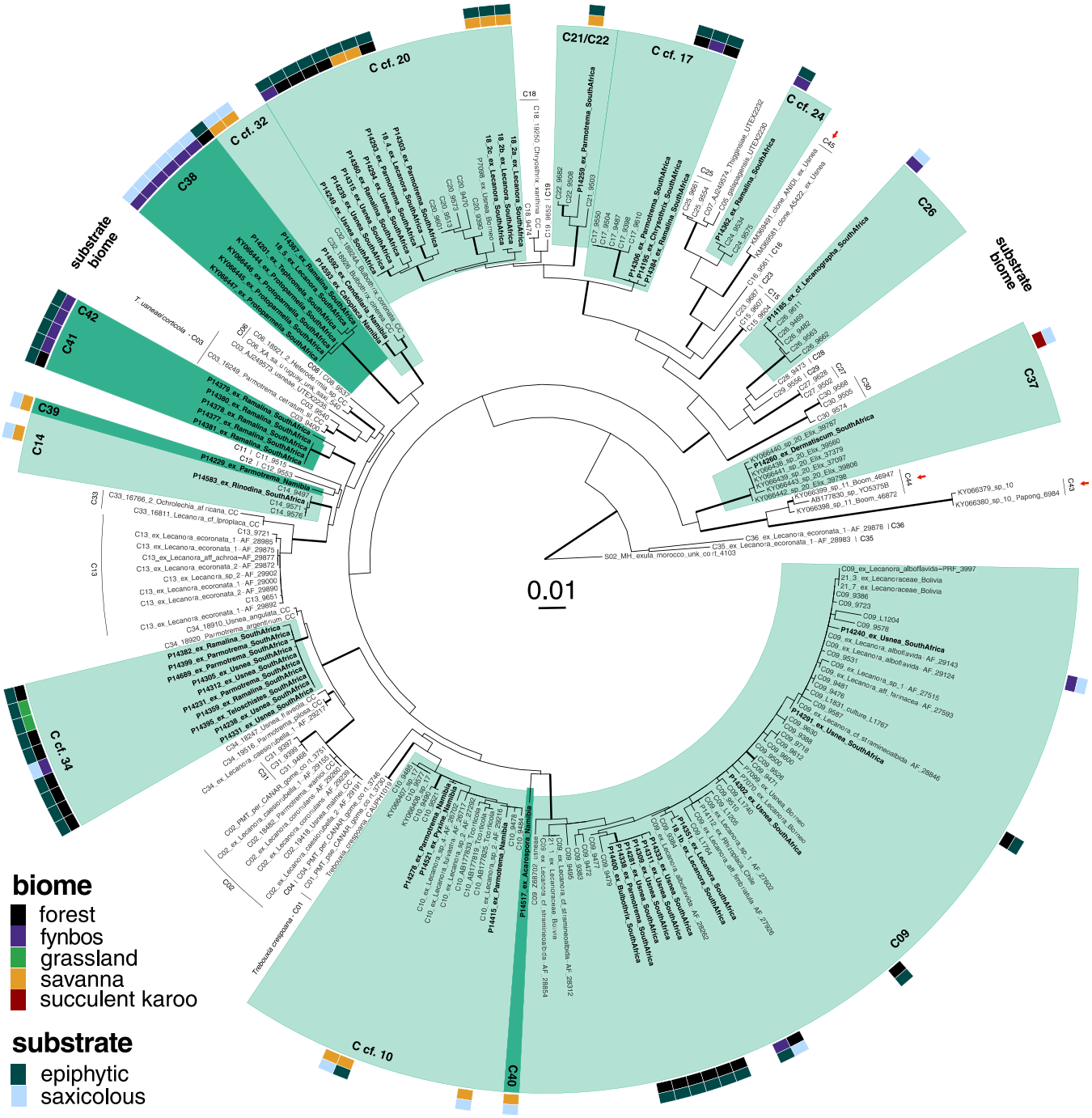


**FIGURE 4** Phylogeny of *Trebouxia* clade C based on maximum likelihood analysis of the concatenated nrITS-*rbcL* (data set A). Thick branches indicate ultrafast bootstrap ≥95%. Samples from southern Africa are indicated with bold text. Putative species-level lineages found in southern Africa are highlighted in green; pale green indicates species known from outside the study region; dark green indicates novel putative species that are potentially endemic to southern Africa. Biome and substrate are indicated in the inner and outer ring, respectively, for southern African samples. *Trebouxia* C43, C44, and C45, indicated with red arrows, do not occur in southern Africa but are incorporated into the *Trebouxia* classification scheme for the first time. Scale indicates substitutions per site. A version of this tree with all ultrafast bootstrap values ≥50% is available in Appendix S9.

novel species. The taxon we designate as *Trebouxia* C37 was previously found in Australia by Singh et al. (2017, as "*Trebouxia* sp. 20") but was omitted from the classification scheme of Muggia et al. (2020). Two highly supported clades, *Trebouxia* C38 and C41, were identified as novel species unique to southern Africa. An additional three singletons were recognized as novel species based on their dissimilarity to new and previously available data. *Trebouxia* C39 had a top nrITS BLAST hit of 92.3% to *T. higginsiae* MK328540 with 99% coverage. *Trebouxia*

C40 had a top nrITS BLAST hit of 94.3% to *Trebouxia* sp. KY066407 from Kenya with 99% coverage. *Trebouxia* C42 had a top nrITS BLAST hit of 92.5% to *Trebouxia* C13 OK533998 with 97% coverage. Apart from our southern African sampling, we found three additional putative species from Buckley et al. (2014) and Singh et al. (2017) that were omitted from the Muggia et al. (2020) classification. These fell outside any currently delimited species (Figure 4) and should be incorporated into the classification as *Trebouxia* C43 ("*Trebouxia* sp. 10" sensu Singh et al. 2017), C44 ("*Trebouxia* sp. 11" sensu Singh et al. 2017), and C45.

Our consensus classification for *Trebouxia* clade I grouped southern African sequences into 11 species (Figure 5). A single sequence was recorded as the novel species *Trebouxia* I32 (top BLAST hit was 94.2% to *T.* sp. KM369745, with 100% coverage). While preparing the alignments for this clade, we found that the recently recognized species I29 (Kosecka et al., 2022) was an artifact caused by the treatment of nrITS and *rbcL* sequences from different *Trebouxia* clades as a single sample. In samples 18308 and 18300 from Kosecka et al. (2022), the nrITS was from Clade I, but the *rbcL* was clade C; for sample 18921, the nrITS was Clade C, but the *rbcL* was Clade I. When just the nrITS was considered, sample 18300 was close to I19, while sample 18308 was conspecific with I28 (Figure 5; Appendix S9).

The only clade S species in our sampling, *Trebouxia* S19 (Appendix S9), was first reported from *Tephromela* in New Zealand by Muggia et al. (2014) and is one of the few *Trebouxia* species previously known from South Africa (Moya et al., 2021). Moya et al. referred to their sample as *T. australis* A. Beck (Beck, 2002), but it is not clear whether that species is conspecific with S19; ultrafast bootstrap support for the clade that included S19, S20, and the type strain of *T. australis* (SAG2205, FJ626726) was 78% (Appendix S9). Apart from the southern African data, we also affirmed that *Trebouxia* S51, a species delimited by Molins et al. (2018) but omitted from Muggia et al. (2020), should be included in the *Trebouxia* classification (Appendix S9). Note that other putative species introduced by Molins et al. (2018) based on partial nrITS sequences were not validated here.

## Evaluation of the "barcode gap"

We analyzed nearly all available *Trebouxia* nrITS sequences to check for a "barcode gap." The final data set included 3392, 714, 1607, and 2344 sequences from clades A, C, I, and S, respectively (data set B, Appendix S10). Distributions of pairwise phylogenetic distances and BLAST similarities had local minima in the region (distance of ca. 0.01–0.05 substitutions/site, ca. 95–99% similarity) where a barcode gap might be expected (Figure 6). However, the distributions were not discontinuous. The number of species recognized by the ASAP barcode gap method varied by an order of magnitude within the top five delimitations (Appendix S12). At the lower bound, ASAP yielded a similar number of species as recognized by 97% OTU clustering (clades A and S) or under the monophyly-known species classification (clade C). At the upper bound, ASAP recognized hundreds more species than any other method.

## Biogeography, endemism, and interbiome species turnover

Analyses of our sampling did not suggest that we have documented the full species diversity of southern African *Trebouxia*. The accumulation curve for the consensus species delimitation did not reach a plateau at the genus level or for individual clades, although clade A and especially clade I may be beginning to level off (Figure 7A). The same pattern was observed when the accumulation curve was calculated for 97% OTU clustering (Appendix S13).

Under the consensus classification, 43 *Trebouxia* species were present in southern Africa, a remarkably similar number to the *Trebouxia* biodiversity documented from Bolivia (44 species) and Kenya (45 species; Figure 7B). Only four *Trebouxia* species were present in all three of the well-sampled southern hemisphere regions (southern Africa, Kenya, and Bolivia), while southern Africa shared 10 and 12 species with Kenya and Bolivia, respectively (Figure 7B). The remaining 17 species include species shared with other regions (e.g., Europe or Australia) and lineages unique to southern Africa. Patterns of shared 97% OTUs were similar (Appendix S13). Southern Africa had greater phylogenetic diversity in *Trebouxia* clade A than either Kenya or Bolivia, but substantially less diversity in clade S (Table 2). For all three regions, Clade C had the highest phylogenetic diversity, but that diversity was lowest in southern Africa. Under the Muggia et al. (2020) classification scheme, the 43 putative *Trebouxia* species in southern Africa represent ca. 30% of global *Trebouxia* diversity, corresponding to ca. 20% of global diversity using 97% OTU clustering (Table 1; Appendix S12), comparable to the proportions of global phylogenetic diversity in clades A, C, and I (Table 2).

Seven putative species—approximately 16% of the *Trebouxia* species observed in our sampling—were novel lineages not known from elsewhere in the world (Figures 3–5). The level of potential endemism rose to ca. 38% under 97% OTU clustering. Novel, potentially endemic *Trebouxia* species were found in 13% of lichen thalli in the Greater Cape Floristic Region under the consensus species delimitation and 31% under 97% OTU clustering (Appendix S14). For the desert, potentially endemic *Trebouxia* species were found in 8% of thalli under the consensus delimitation and 15% under 97% OTU clustering. In all four cases, the percentage of putative endemics was not significantly greater than a null distribution (GCFR-consensus, $P = 0.283$; GCFR-97%, $P = 0.210$; desert-consensus, $P = 0.813$; desert-97%, $P = 0.970$; Appendix S14).

Of the three bioclimatic variables (MAT, MAP, and precipitation seasonality) evaluated for their relationship to variation in *Trebouxia* community composition, only MAP

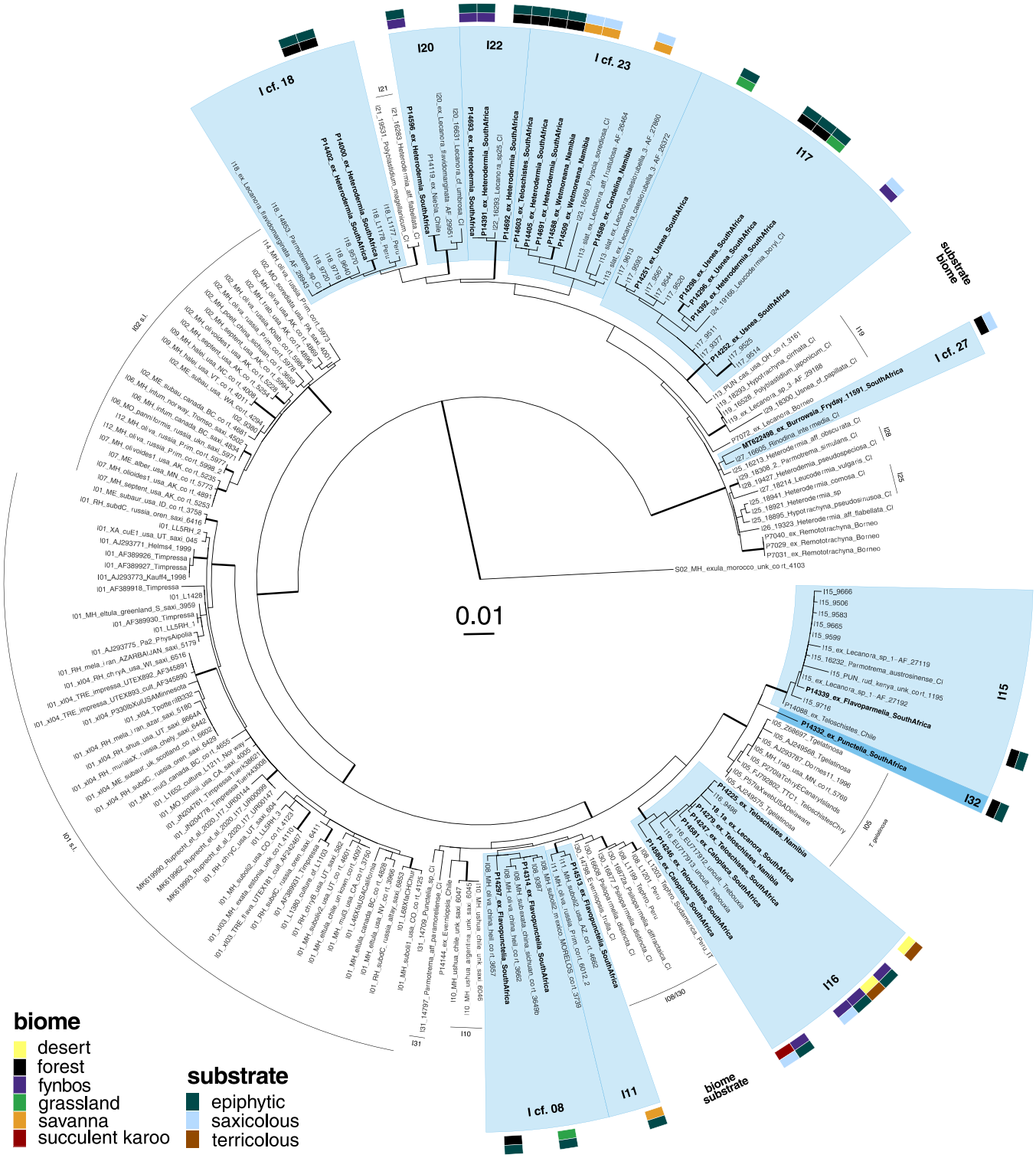


**FIGURE 5** Phylogeny of *Trebouxia* clade I based on maximum likelihood analysis of the concatenated nrITS-*rbcL* (data set A). Thick branches indicate ultrafast bootstrap ≥95%. Samples from southern Africa are indicated with bold text. Putative species-level lineages found in southern Africa are highlighted in blue; pale blue indicates species known from outside the study region; dark blue indicates a novel putative species that is potentially endemic to southern Africa. Biome and substrate are indicated in the inner and outer ring, respectively, for southern African samples. Scale indicates substitutions per site. A version of this tree with all ultrafast bootstrap values ≥ 50% is available in Appendix S9.

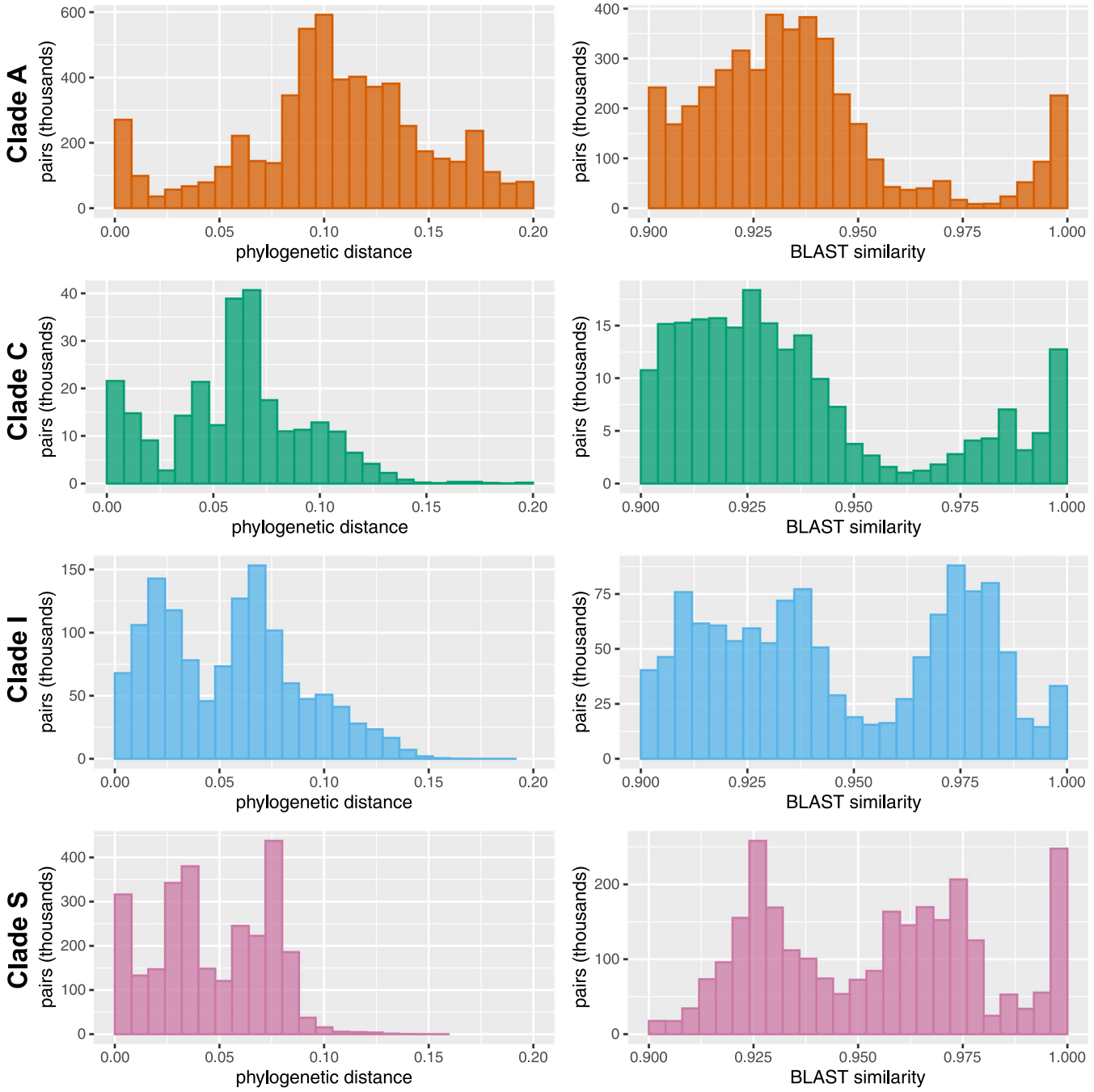


**FIGURE 6** Absence of a "barcode gap" in *Trebouxia* nrITS sequences (data set B). For each major clade, pairwise phylogenetic distances in substitutions per site are shown on the left and pairwise BLAST sequence similarities as a fraction of sequence length are shown on the right. Phylogenetic distances greater than 0.2 or BLAST similarities less than 0.9 were omitted to enable uniform comparison across clades. Although both measures have local minima in the region where a gap might be expected, there is no discontinuity.

was a significant explanation of variation at all levels of classification (Table 3). MAT was only weakly significant for 97% OTUs, and seasonality was not significant at any level. *Trebouxia* clades A, C, and I were found throughout the study area, while clade S was only found in the Cape Floristic Region (Appendix S15). The driest sites (desert and succulent karoo) lacked clade C and were dominated by clade A, while clade I was least common in arid and savanna sites (Figure 8A; Appendix S15). Many *Trebouxia* species occurred in multiple biomes, and all sites shared at least one species with another site (Figure 8A). Photobiont ranges that cross biomes followed a consistent pattern: desert and succulent karoo shared *Trebouxia* species with fynbos; fynbos shared *Trebouxia* species with the arid biomes and with forest and grassland. Savanna only shared *Trebouxia* species with forest and grassland, with one exception: C cf. 20, also shared with fynbos (Figure 8A). Notably, the savanna sites at the northeastern (Kruger) and northwestern

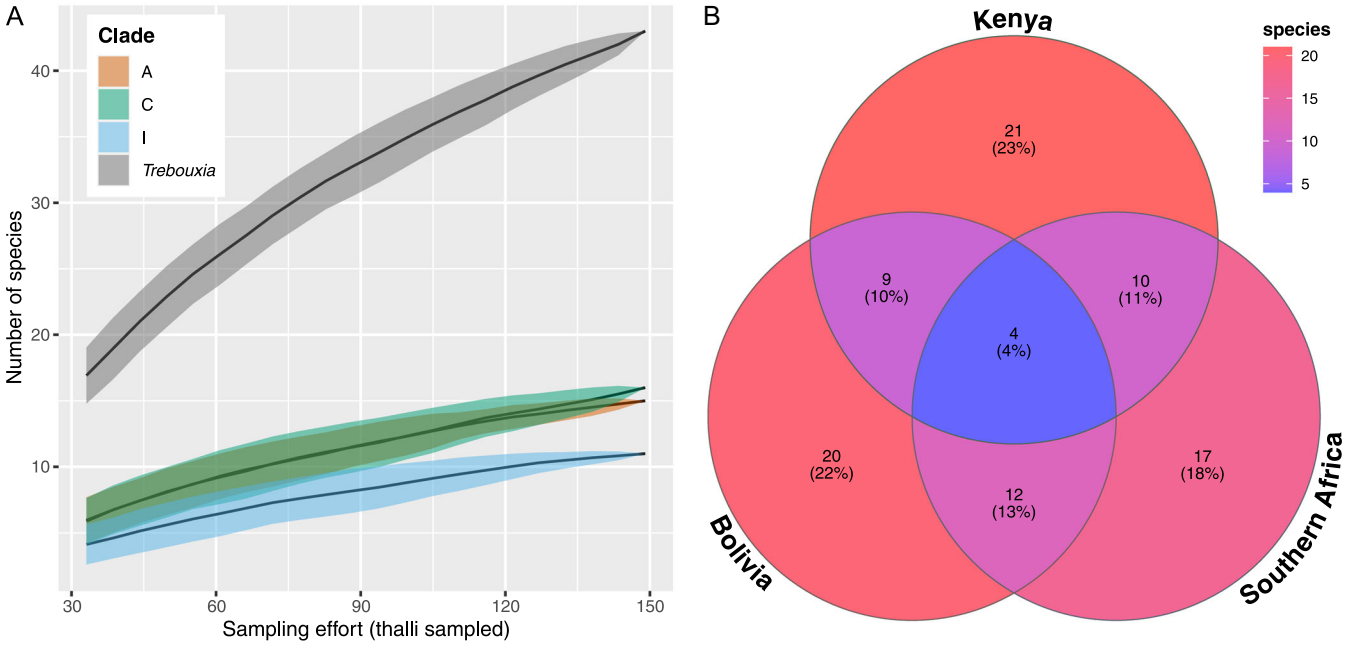


**FIGURE 7** (A) Species accumulation curves for southern African *Trebouxia* based on the consensus delimitation (Figures 3–5). An accumulation curve was not calculated for clade S because only a single species from that clade was recorded in the study region. (B) Counts of *Trebouxia* species shared between southern Africa and the best-sampled regions in South America and Africa: Bolivia (507 samples; Lutsak et al., 2016; Medeiros et al., 2021; Kosecka et al., 2022) and Kenya (146 samples; Leavitt et al., 2015; Lutsak et al., 2016; Singh et al., 2017; Muggia et al., 2014, 2020). New Zealand also has a high number of available *Trebouxia* nrITS sequences, but these are almost all from a single mycobiont genus (Buckley et al., 2014). A version of this figure based on 97% OTU clustering is included as Appendix S13.

**TABLE 2** Proportion of global *Trebouxia* phylogenetic diversity for each major clade observed in the three best sampled regions of the southern Hemisphere (excluding Antarctica), based on the trees from data set B. Branch lengths represent substitutions per site.

| Clade | Total length | Southern Africa | Kenya | Bolivia |
|---|---|---|---|---|
| A | 6.22 | 0.192 | 0.125 | 0.133 |
| C | 2.52 | 0.243 | 0.335 | 0.358 |
| I | 2.29 | 0.189 | 0.113 | 0.230 |
| S | 1.92 | 0.004 | 0.027 | 0.076 |

**TABLE 3** Results of adonis2 PERMANOVA on the influence of mean annual temperature (BIO1), mean annual precipitation (BIO12), and precipitation seasonality (BIO15) on the composition of *Trebouxia* communities. Variables that were significant at $P \leq 0.05$ are in bold.

| *Trebouxia* classification level | BioClim variable | $R^2$ | *F* | *P* |
|---|---|---|---|---|
| Clades | BIO1 | 0.05746 | 0.9691 | 0.457 |
| | **BIO12** | **0.26711** | **4.5048** | **0.004** |
| | BIO15 | 0.08247 | 1.3908 | 0.240 |
| Consensus species | BIO1 | 0.09056 | 1.3208 | 0.129 |
| | **BIO12** | **0.15864** | **2.3137** | **0.001** |
| | BIO15 | 0.06513 | 0.9499 | 0.531 |
| 97% OTUs | **BIO1** | **0.10261** | **1.4370** | **0.045** |
| | **BIO12** | **0.12223** | **1.7117** | **0.004** |
| | BIO15 | 0.06106 | 0.8551 | 0.716 |

(Waterberg) ends of our sampling did not share any photobiont species (Figure 8A).

Closeness and betweenness metrics confirmed the visual impression that forest and fynbos sites are central to photobiont community connectivity across biomes (Figure 8A; Appendices S16 and S17). The Buffelskloof (forest) and West Coast (fynbos) sites had the highest empirical values for normalized betweenness and closeness. These were also the sites with the most samples, and both metrics were significantly correlated with sampling depth in a linear regression (betweenness, $R^2 = 0.6439$, F = 24.51, df = 12, P = 0.0004; closeness, $R^2 = 0.4255$, $F = 10.63$, df = 12, $P = 0.0068$). However, our resampling and null model analyses suggested that the centrality of these sites may not be entirely an artifact of sampling depth. In the rarefaction/resampling test, Buffelskloof and West Coast remained among the most central sites (Appendix S16). Buffelskloof and West Coast were also the most central sites in the randomized/null test, but for these two sites and others with high empirical normalized betweenness, nearly all betweenness values in the null simulation were lower than the empirical values (Appendix S16).

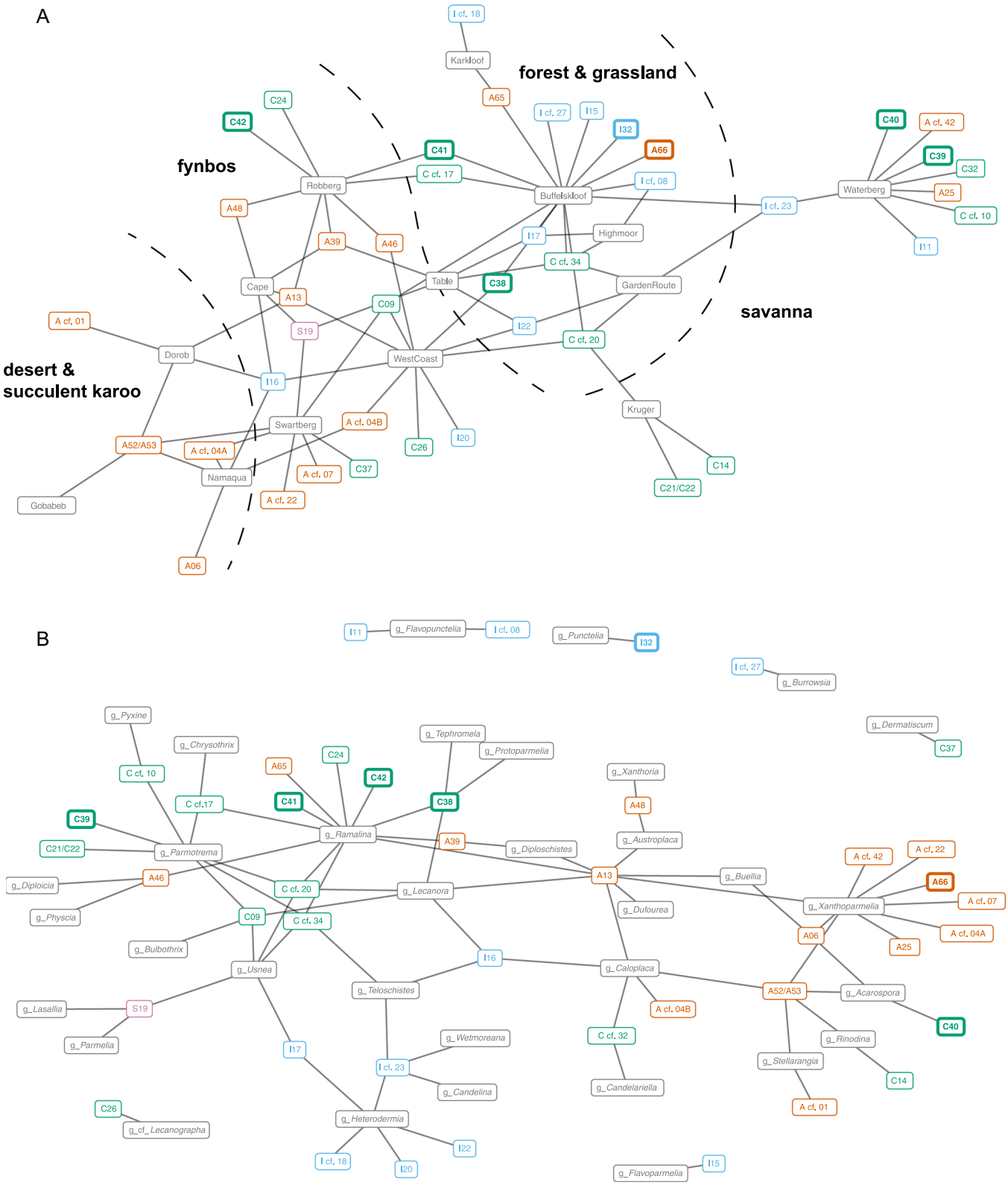


**FIGURE 8** (A) Site–photobiont network of localities sampled for this study. (B) Mycobiont–photobiont network. Note that lichen-forming fungi (mycobionts) are grouped at the genus rank. Both networks are based on the consensus *Trebouxia* classification (Figures 3–5). Photobiont labels are colored by major clade (Appendix S2) and potentially endemic *Trebouxia* species are shown in bold. A version of this figure based on 97% OTU clustering is included as Appendix S17.

## Specificity and generalism in the lichen symbiosis

At the level of lichen thalli, more variation in photobiont consensus species identity was explained by mycobiont genus (df = 31, $R^2 = 0.250$, $P = 0.001$) than site (df = 13, $R^2 = 0.078$, $P = 0.951$) or biome (df = 1, $R^2 = 0.007$, $P = 0.385$). However, while mycobiont genus was a significant predictor of photobiont species, it still only explained a minority of the variation in photobiont species among lichen thalli. Mycobiont genera varied widely in their specificity. On one end of the spectrum, some were exclusively associated with a single *Trebouxia* clade (Figure 8B), e.g., *Heterodermia* Trevis. and clade I ($N = 9$), *Lasallia* Mérat and clade S ($N = 3$), *Parmotrema* A. Massal. and clade C ($N = 11$), and *Xanthoparmelia* and clade A ($N = 18$). *Heterodermia*, *Parmotrema*, and *Xanthoparmelia* were each associated with multiple photobiont species within their respective clades; only a single species was found for *Lasallia* in clade S (Figure 8B).

In contrast, *Usnea* Dill. ex Adans. and *Caloplaca* Th. Fr. were associated with *Trebouxia* clades C, I, and S. Several mycobiont genera were found with photobionts from both clades A and C—*Acarospora* A. Massal., *Buellia* De Not., *Lecanora* Ach., and *Ramalina* Ach.—while *Teloschistes* Norman occurred with clades C and I (Figure 8B). While few mycobiont species were well-represented in our sampling, species with multiple collections tended to follow the genus pattern and not show a higher level of specificity. *Heterodermia leucomelos* (L.) Poelt s.l. [including *H. boryi* (Fée) Kr.P. Singh & S.R. Singh; $N = 5$ across three sites] was associated with three *Trebouxia* species: I20, I22, and I cf. 23 (Appendix S4), while *Ramalina celastri* (Spreng.) A. Massal. ($N = 5$ across three sites), was associated with four *Trebouxia* species (Appendix S4). Within each biont, higher values for degree and normalized betweenness centrality suggested generalists that were important to the overall structure of the network. For mycobionts, the most important generalist genera according to these metrics were *Ramalina*, *Xanthoparmelia*, *Caloplaca*, *Usnea*, and *Lecanora* (Appendix S17; all values from the network with the consensus species delimitation). Aside from *Xanthoparmelia*, which occurred with many different species in *Trebouxia* clades A, these genera were associated with multiple clades of *Trebouxia*.

The modularity of the empirical mycobiont–photobiont network was not significantly different from the null distribution (Appendix S18; $P = 0.064$). Nestedness was significantly lower than the null distribution (i.e., showing an anti-nested pattern) for mycobionts ($P = 0.000$) and photobionts ($P = 0.022$). Ranked by betweenness centrality, *Trebouxia* A13 was the most important generalist photobiont (degree = 8, normalized betweenness = 0.318), followed by C cf. 34, A52/A53, C cf. 20, and I cf. 23 (Appendix S19). Except for C cf. 34, these are also species that exhibited conflict between delimitation methods (Appendix S11), calling into question whether some of this apparent generalism was biodiversity missed by the consensus classification. The mycobiont–photobiont network with *Trebouxia* species delimited under 97% OTU clustering (Appendix S17) suggested otherwise: The OTU representing most specimens in A13 still had the highest betweenness centrality, with three of the next four spots filled by OTUs linked to other species listed above (Appendix S19). It is important to note that these centrality metrics were also significantly associated with the number of samples (linear regression: betweenness-consensus, $R^2 = 0.738$, $F = 119$, df = 41, $P < 0.0001$; betweenness-97%, $R^2 = 0.529$, $F = 65$, df = 56, $P < 0.0001$).

# DISCUSSION

## *Trebouxia* in southern Africa

Although recent advances have brought considerable order to the molecular-era taxonomy of *Trebouxia* (Leavitt et al., 2015; Muggia et al., 2020), many putative species are known from only one or a handful of sequences, and many areas of the world lack data, particularly in the southern hemisphere. Before the present study, Kenya was the only country in sub-Saharan Africa where the *Trebouxia* biota was extensively documented with sequence data (Lutsak et al., 2016; Muggia et al., 2020). Our study provides a first attempt at a comprehensive survey of *Trebouxia* in South Africa and Namibia. Documenting photobiont diversity in this region is important not just for *Trebouxia* systematics, but also for informing studies of lichen physiology in arid environments. Past physiological studies on lichen photosynthesis in southern Africa (e.g., Wessels and Kappen, 1993; Lange et al., 1994; Maphangwa et al., 2012) have not included a species identification for the photobiont—the organism that is photosynthesizing. With the framework from our study, future work on lichen physiology in this region can be linked to *Trebouxia* species.

Our collecting strategy was to sample from a wide diversity of lichens and habitats; most vegetation types and mycobiont species were only sampled once or twice. This approach allowed us to assess overall *Trebouxia* biodiversity and patterns at an interbiome scale, but it limits our ability to investigate intrabiome patterns, evaluate photobiont specificity at the level of mycobiont species, or explore the ecological preferences of individual *Trebouxia* species. One such limitation can be seen in the interpretation of the species accumulation curve (Figure 7): We cannot be sure whether the results are due to undiscovered species or insufficient within-habitat replicates. In addition, the high proportion of singletons (ca. 40% using the consensus classification) makes our data set unsuitable for nonparametric estimates of the species pool (Lopez et al., 2012). Despite this uncertainty, the phylogenetic diversity of sampled photobionts and mycobionts—representing the four largest clades in *Trebouxia* and many families of lichen-forming fungi—and comparable *Trebouxia* biodiversity to Bolivia and Kenya suggest that our data set, if not complete, is reasonably comprehensive and acceptable for further analyses.

If the putative endemic species—ca. 16% of the regional *Trebouxia* biota—found in our sampling are indeed regional endemics, it would suggest that *Trebouxia* follows some of the biogeographic "rules" of southern Africa but not others. *Trebouxia* appears to conform to a plant- and lichen-informed expectation that there will be endemism in southern Africa, but those putative endemic species were not where we expected to find them, i.e., not preferentially associated with the Greater Cape Floristic Region or desert. To the contrary, we saw a trend toward lower desert endemism than expected by chance (Appendix S14), although this was not significant when correcting for multiple comparisons. In further contrast with plants and lichenized fungi, there was no evidence that the putative endemic species in *Trebouxia* clade C represent a radiation, although the low backbone support (Figure 4) did not eliminate that possibility. The novel species hypothesized to be regional endemics in this study were mostly singletons (Figures 3–5), and additional data from southern Africa, Australia, and other biogeographically related areas will allow us to better understand the ecological and geographic breadth of these species and assess whether they are truly endemic. In this context, the potential for a *Trebouxia* biota shared between Mediterranean biomes deserves greater study. *Trebouxia maresiae* (A46) was previously known from Teloschistaceae and *Ramalina* in the western Mediterranean and Cape Verde archipelago (Gasulla et al., 2010; Nyati et al., 2014; Garrido-Benavent et al., 2022). In our study, it was found in the fynbos biome with Caliciaceae, Physciaceae, and Ramalinaceae (Figure 3, 8), clearly marking it as an inhabitant of Mediterranean habitats while also expanding its geographic and partner breadth—an example of how endemism can be a figment of limited sampling.

The effect of annual precipitation on *Trebouxia* community composition observed in this study (Table 3) has been previously observed at multiple spatial scales (Singh et al., 2017; Wagner et al., 2021). Despite its central role in structuring the plant communities of the Greater Cape Floristic Region, precipitation seasonality had no significant effect on community composition in southern African *Trebouxia* (Table 3). This result is not necessarily surprising, given that desiccation tolerance in both the lichenized and free-living states is a hallmark of *Trebouxia* (Candotto Carniel et al., 2015). However, our selection of sampling locations may have concealed effects of precipitation seasonality. Collection sites in the winter rainfall region were all near the coast, where *Trebouxia*-associated lichens can rehydrate from ocean mist or water vapor in humid air (Lange et al., 1986). Future research should document the *Trebouxia* biota of inland winter rainfall sites to evaluate whether the absence of a seasonality effect still holds true.

Other ecological patterns in our data echo trends previously seen in *Trebouxia* or southern African vegetation. The dominance of *Trebouxia* clade A on the coast of Namibia (Appendix S15) has also been observed in the Atacama desert, another low-precipitation, fog-driven environment (Vargas Castillo and Beck, 2012). The prominence of clade A in such environments may explain why phylogenetic diversity of this clade is higher in Southern Africa than in Bolivia or Kenya (Table 2). The absence of hard boundaries in species composition between biomes—evident in the structure of the photobiont–site network (Figure 8A) and the poor ability of biome to explain variation in photobiont species—is a reminder that species turnover is an individualistic process observed at the community level (Whittaker, 1960). All major biomes in southern Africa share some plant species (Gibbs Russell, 1987), which is largely true for *Trebouxia*, although we have yet to find species shared between desert and savanna. Future studies in this region should conduct more thorough intrabiome sampling of *Trebouxia* to quantify relative species turnover within and between biomes. Sampling of the Nama-karoo and Albany thicket, biomes that were missing from our data set and are biologically under-sampled more generally (Hoveka et al., 2020), will also be required to fully understand the distribution of *Trebouxia* species.

## Mycobiont–photobiont specificity in *Trebouxia*-associated lichens

Our data confirmed patterns of mycobiont–photobiont specificity that have been seen elsewhere in the world. Kosecka et al. (2022) found *Heterodermia* in Bolivia almost always associated with *Trebouxia* clade I; this clade also appears to be the exclusive source of photobionts for *Punctelia* and relatives (Garrido-Benavent et al., 2023). The association between *Lasallia* and *Trebouxia* clade S has been seen in numerous studies (Sadowska-Deś et al., 2013, 2014; Hestmark et al., 2016; Dal Grande et al., 2018; Paul et al., 2018; Rolshausen et al., 2020), as has the association between *Parmotrema* and *Trebouxia* clade C (Ohmura et al., 2006; Škaloud et al., 2018; Ohmura et al., 2019; Kosecka et al., 2022). The latter association might explain the high proportion of temperate *Parmotrema* species producing soredia alone or in addition to apothecia (Lawrey, 1980) because clade C is primarily tropical and thus less likely to be encountered by a germinating *Parmotrema* ascospore in temperate environments. One striking observation was that clades particularly rich in endemic mycobiont species (*Xanthoparmelia* and Teloschistaceae) were rarely associated with novel *Trebouxia* species (Figure 8B), suggesting a lack of co-speciation between the fungal and algal partners in the lichen symbiosis.

The modularity of the mycobiont–photobiont network was marginally not significant in our analysis (Appendix S18). It is possible that a significant modular structure would be evident if the network were inferred with mycobionts at the rank of species rather than genus, and future work should increase the sampling of southern African lichens to enable such an analysis. Our finding of significant anti-nested network structure for both mycobionts and photobionts is consistent with previous work on lichens (Chagnon et al., 2018; Pérez-Ortega et al., 2023), and, along with the finding that mycobiont genus is a significant predictor of photobiont species, supports a role for both

interaction specificity and environment in structuring lichen photobiont communities.

## *Trebouxia* biodiversity worldwide

Our results refined and expanded the global *Trebouxia* classification scheme (Leavitt et al., 2015; Muggia et al., 2020). We added 12 new species to this classification, seven of which are potentially endemic to southern Africa. Four of the 12 species were previously recorded by Singh et al. (2017) but were omitted from the classification scheme until now: C37 ("*Trebouxia* sp. 20"), C38 ("*Trebouxia* sp. 18", a potential southern African endemic), C43 ("*Trebouxia* sp. 10"), and C44 ("*Trebouxia* sp. 11"). Conversely, we rejected *Trebouxia* I29 (proposed by Kosecka et al., 2022) as a phylogenetic artifact caused by nrITS and *rbcL* sequences from different *Trebouxia* clades, likely due to multiple algal species in a single thallus. We also resolved a problem with *Trebouxia* A29, which was paraphyletic in previous papers that inferred trees from nrITS and *rbcL* (e.g., Muggia et al., 2020) but was recovered as a single clade in trees based on nrITS only (e.g., Muggia et al., 2014). We found that the former topology was due to two samples with *rbcL* matching a different species, *Trebouxia* A13.

Although the distributions of pairwise distances and sequence similarities suggest, unsurprisingly, that intra- and interspecific distances are different, the lack of a discontinuity (Figure 6) means that there is no "barcode gap" in *Trebouxia*. The highly inconsistent number of species recognized under the top ASAP partitions (Appendix S12) is a consequence of the lack of a gap. Beyond the violation of the assumption that a gap exists, there is a methodological mismatch at play here. The "barcode gap" approach is ideal for clades that are "taxonomically well-understood and thoroughly sampled" (Meyer and Paulay, 2005). *Trebouxia* is neither: it is insufficiently sampled, and species boundaries are poorly known independent of molecular data. Apparent gaps may just be due to species that are known from one or two specimens. Additional sampling will likely reduce the appearance of a gap, as highlighted by C21/C22 (Figure 4). These were recognized as two distinct species by Muggia et al. (2020) based on nrITS distances. Our sequence falls in the middle of that nrITS "gap", and this clade may represent a single species.

The absence of a barcode gap does not mean that the existing classification scheme, which delimited species based primarily on a barcode gap analysis, needs to be discarded. Indeed, the species of that scheme are generally monophyletic entities (Figures 3–5) and often consistent with those of other delimitation approaches (Appendices S10 and S11). Thus, despite inherent limitations of the barcode gap approach, the analyses from Leavitt et al. (2015) and Muggia et al. (2020) were a good initial effort to delimit potential species. What our barcode gap analysis does show is that it is not possible to define species in *Trebouxia* based on a single distance or similarity threshold, either across the entire genus or within a major clade. Without a gap, any threshold is arbitrary. Absent data other than nrITS and specimen vouchers, the best option is to define species based on well-supported phylogenetic relationships and informed by ecology (Wiemers and Fiedler, 2007; Malavasi et al., 2016). Because *Trebouxia* species delimited through a barcode gap approach may not consistently reflect natural species boundaries, our results also highlight that it is important to use multiple delimitation approaches to ensure that ecological analyses are robust to errors or subjective decisions in species delimitation.

Studies such as this one, which apply provisional names to *Trebouxia* species delimited with just one or a few loci, provide a starting framework that should be expanded in future genomic and morphological research. For example, Muggia et al. (2020) recognized *Trebouxia* A36 as a South African singleton sister to the widespread A13, while in our analysis, A36 was nested within A13 (Figure 3). This clade is characterized by an intron in ITS1 not found in any other *Trebouxia* species. There are three names available for A13—*T. arboricola* Puymaly, *T. crenulata* Archibald, and *T. aggregata* (Archibald) Gärtner (Muggia et al., 2020), which have some morphological differences among them (Bordenave et al., 2022). Resolving species boundaries in this lineage will require genomic and morphological work in parallel. Another example is the A52/A53 clade (Figure 3), which contains *Trebouxia* from deserts, mountaintops, and other extreme environments in South America and southern Africa (Ruprecht et al., 2020; Medeiros et al., 2021; De Carolis et al., 2022). We leave the question of whether this represents a single, widely distributed, extremophile species or many narrowly distributed species unresolved until we have more comprehensive data.

While the nomenclatural scheme from Leavitt et al. (2015) and Muggia et al. (2020) has found widespread acceptance, its informal nature presents problems that must be addressed as its usage grows. From a practical standpoint, the lack of a central registry for sequential, alphanumeric species identifiers makes it almost certain that the same "name" will be published more or less simultaneously for different species. This duplication has already happened: Ruprecht et al. (2020) introduced several novel *Trebouxia* species contemporaneously with Muggia et al. (2020), and "A36," "A37," "A38," "A39," "I17," and "S16" sensu Ruprecht et al. (2020) do not correspond to the taxa with the same names published by Muggia et al. (2020; Appendix S20). We make two suggestions to avoid this situation in the future. First, publications delimiting new putative species in *Trebouxia* should state that explicitly. Second, the community working on *Trebouxia* systematics should agree on a system that will allow authors to "reserve" identifiers for publications in press.

## CONCLUSIONS

With a phylogenetic framework and classification scheme for *Trebouxia* now well established, studies that need to identify *Trebouxia* species can use phylogeny-based delimitation with

tools such as T-BAS (Carbone et al., 2017, 2019). If phylogeny-based methods are not possible, it is preferable to define species based on a threshold acknowledged to be arbitrary, such as clustering OTUs at 97%, rather than applying "barcode gap" methods whose central assumption—that a gap exists—is not met in *Trebouxia*. Investigating ecological questions with multiple approaches to species delimitation, as we did here, can be a way to increase confidence in conclusions when species boundaries are uncertain.

This study provides a first step toward documenting the biodiversity, biogeography, and ecology of *Trebouxia* in southern Africa, a region that hosts ca. 20–30% of global *Trebouxia* biodiversity. Only ca. 12% of the putative *Trebouxia* species found in our sampling can be referred to formally described species, leaving dozens of taxa—including all the potential southern African endemics—remaining to be described. Our data on habitats and fungal partners for these species provide a blueprint for a targeted effort to collect, culture, and describe these algae, adding another layer to our understanding of biodiversity in South Africa and Namibia.

## AUTHOR CONTRIBUTIONS

I.D.M.: conceptualization, methodology, software, formal analysis, investigation, data curation, writing original draft, review and editing, visualization; A.I.: project administration, review and editing; A.E.A.: investigation, review and editing, project administration, funding acquisition; T.A.H.: investigation, resources, review and editing; J.M.: investigation, data curation, review and editing, supervision, project administration, funding acquisition; A.F.: investigation, review and editing; I.C.: software, review and editing, funding acquisition; S.L.G.: investigation, data curation, review and editing; N.M.: investigation, review and editing; E.M.: investigation, review and editing; R.V.C.: investigation, review and editing; J.G.: investigation, review and editing; M.K.: investigation, review and editing; G.M.K.: resources, review and editing; S.O.: investigation, review and editing; J.S.S.S.: resources, review and editing; E.T.: investigation, review and editing; E.F.Y.H.: investigation, review and editing; L.A.L.: investigation, review and editing; F.L.: conceptualization, methodology, investigation, review and editing, supervision, project administration, funding acquisition. All authors have read and agreed to the published version of the manuscript.

## ACKNOWLEDGMENTS

Specimens were collected and exported under permits from South African National Parks (CRC/2019-2020/020-–2018/V1), Ezemvelo KZN Wildlife (OP 1404/2019), Mpumalanga Parks and Tourism Agency, CapeNature (CN35-31-9213 and export permit CN17-31-9607), and the Namibian Ministry of Environment and Tourism. We thank the Namibian National Botanical Research Institute (NBRI) and National Commission on Research, Science and Technology. We acknowledge the Sabah Biodiversity Center (SABC) and Sabah Parks for issuing collecting and export permits in Borneo [Access License JKM/MBS.1000-2/2 JLD.6 (101) and Transfer License JKM/MB.1000-2/3 JLD.3 (70)] and the Corporación Nacional Forestal for issuing collecting and export permits in Chile (034/2016). Funding for this research was provided by the United States National Science Foundation (NSF) through the collaborative grant "GoLife: Filling the largest void of the fungal genealogy of life (the Pezizomycotina) and integrating symbiotic, environmental and physiological data layers" (DEB 1541548 to F.L. and J.M.; DEB 1541496 to A.E.A.; DEB 1541538 to E.F.Y.H.). I.D.M. was supported by an NSF Graduate Research Fellowship under grant DGE 1644868. The authors thank Carlos Pardo-De la Hoz, Shannon Skarha, Diego Garfias Gallegos, and Pierre-Luc Chagnon for feedback on an initial draft and thank Silke Werth and three anonymous reviewers for comments that improved the manuscript.

## DATA AVAILABILITY STATEMENT

Molecular sequences generated in this study have been submitted to GenBank (accession numbers are listed in Appendices S4–S6). All multiple sequence alignments and tree files are available on FigShare (doi: 10.6084/m9.figshare.c.6661265), and we have updated the *Trebouxia* phylogenies on T-BAS with the results of this paper. As a resource for the community, Appendix S10 includes both the OTU clustering and a preliminary classification in the Muggia et al. (2020) framework for almost all *Trebouxia* nrITS sequences on GenBank. All R scripts used for data analysis and visualization and the raw data files required to run those scripts are available at https://github.com/IanDMedeiros/african-trebouxia. Voucher specimens have been or will be accessioned at DUKE, KRAM, ARIZ, BOL, PRE, and WIND.

## ORCID

*Ian D. Medeiros* http://orcid.org/0000-0003-2179-0745
*Alicia Ibáñez* http://orcid.org/0000-0002-3724-838X
*A. Elizabeth Arnold* http://orcid.org/0000-0002-7013-4026
*Terry A. Hedderson* http://orcid.org/0000-0002-3537-6599
*Jolanta Miadlikowska* http://orcid.org/0000-0002-5545-2130
*Adam Flakus* http://orcid.org/0000-0002-0712-0529
*Ignazio Carbone* http://orcid.org/0000-0003-2721-6656
*Scott LaGreca* http://orcid.org/0000-0002-1988-0437
*Nicolas Magain* http://orcid.org/0000-0001-5409-9518
*Edyta Mazur* http://orcid.org/0000-0003-2628-5473
*Reinaldo Vargas Castillo* http://orcid.org/0000-0003-0064-831X
*József Geml* http://orcid.org/0000-0001-8745-0423
*Gillian Maggs-Kölling* http://orcid.org/0000-0003-3296-8553
*Shuzo Oita* http://orcid.org/0000-0002-0278-9944
*Jaya Seelan Sathiya Seelan* http://orcid.org/0000-0002-0045-6206
*Elizaveta Terlova* http://orcid.org/0000-0001-6029-2445
*Erik F. Y. Hom* http://orcid.org/0000-0003-0964-0031

*Louise A. Lewis* http://orcid.org/0000-0003-0695-5134
*François Lutzoni* http://orcid.org/0000-0003-4849-7143

## REFERENCES

Allaire, J., C. Gandrud, K. Russell, and C. Yetman. 2017. networkD3: D3 JavaScript Network Graphs from R. R package version 0.4. Website: https://CRAN.R-project.org/package=networkD3

Almborn, O. 1988. Some distribution patterns in the lichen flora of South Africa. *Monographs in Systematic Botany from the Missouri Botanical Garden* 25: 429–432.

Almborn, O. 1989. Revision of the lichen genus *Teloschistes* in central and southern Africa. *Nordic Journal of Botany* 8: 521–538.

Almeida-Neto, M., and W. Ulrich. 2011. A straightforward computational approach for measuring nestedness using quantitative matrices. *Environmental Modelling & Software* 26: 173–178.

Baas Becking, L. G. M. 1934. Geobiologie of inleiding tot de milieukunde. W.P. Van Stockum & Zoon, The Hague, Netherlands.

Barreno, E., L. Muggia, S. Chiva, A. Molins, C. Bordenave, F. García-Breijo, and P. Moya. 2022. *Trebouxia lynnae* sp. nov. (Former *Trebouxia* sp. TR9): Biology and biogeography of an epitome lichen symbiotic microalga. *Biology* 11: 1196.

Beck, A. 2002. Selektivität der symbionten schwermetalltoleranter flechten. Ph.D. thesis, Ludwig Maximilian University of Munich, Munich, Germany.

Beckett, S. J. 2016. Improved community detection in weighted bipartite networks. *Royal Society Open Science* 3: 140536.

Bengtsson-Palme, J., M. Ryberg, M. Hartmann, S. Branco, Z. Wang, A. Godhe, P. De Wit, et al. 2013. Improved software detection and extraction of ITS1 and ITS2 from ribosomal ITS sequences of fungi and other eukaryotes for analysis of environmental sequencing data. *Methods in Ecology and Evolution* 4: 914–919.

Berger, S. A., D. Krompass, and A. Stamatakis. 2011. Performance, accuracy, and web server for evolutionary placement of short sequence reads under maximum likelihood. *Systematic Biology* 60: 291–302.

Botnen, S. S., M. L. Davey, R. Halvorsen, and H. Kauserud. 2018. Sequence clustering threshold has little effect on the recovery of microbial community structure. *Molecular Ecology Resources* 18: 1064–1076.

Bordenave, C. D., L. Muggia, S. Chiva, S. D. Leavitt, P. Carrasco, and E. Barreno. 2022. Chloroplast morphology and pyrenoid ultrastructural analyses reappraise the diversity of the lichen phycobiont genus *Trebouxia* (Chlorophyta). *Algal Research* 61: 102561.

Born, J., H. P. Linder, and P. Desmet. 2007. The Greater Cape Floristic Region. *Journal of Biogeography* 34: 147–162.

Buckley, H. L., A. Rafat, J. D. Ridden, R. H. Cruickshank, H. J. Ridgway, and A. M. Paterson. 2014. Phylogenetic congruence of lichenised fungi and algae is affected by spatial scale and taxonomic diversity. *PeerJ* 2: e573.

Câmara, P. E. A. S., F. A. C. Lopes, F. L. V. Bones, L. A. C. Rodrigues, M. Carvalho-Silva, M. Stech, P. Convey, and L. H. Rosa. 2023. Investigating aerial diversity of non-fungal eukaryotes across a 40° latitudinal transect using DNA metabarcoding. *Austral Ecology* 48: 1178–1194.

Candotto Carniel, F., D. Zanelli, S. Bertuzzi, and M. Tretiach. 2015. Desiccation tolerance and lichenization: a case study with the aeroterrestrial microalga *Trebouxia* sp. (Chlorophyta). *Planta* 242: 493–505.

Carbone, I., J. B. White, J. Miadlikowska, A. E. Arnold, M. A. Miller, F. Kauff, J. M. U'Ren, et al. 2017. T-BAS: Tree-Based Alignment Selector toolkit for phylogenetic-based placement, alignment downloads, and metadata visualization: an example with the Pezizomycotina tree of life. *Bioinformatics* 33: 1160–1168.

Carbone, I., J. B. White, J. Miadlikowska, A. E. Arnold, M. A. Miller, N. Magain, J. M. U'Ren, and F. Lutzoni. 2019. T-BAS version 2.1: Tree-Based Alignment Selector toolkit for evolutionary placement and viewing of alignments and metadata on curated and custom trees. *Microbiology Resource Announcements* 8: e00328-19.

Chagnon, P. L., N. Magain, J. Miadlikowska, and F. Lutzoni. 2018. Strong specificity and network modularity at a very fine phylogenetic scale in the lichen genus *Peltigera*. *Oecologia* 187: 767–782.

Chernomor, O., A. Von Haeseler, and B. Q. Minh. 2016. Terrace aware data structure for phylogenomic inference from supermatrices. *Systematic Biology* 65: 997–1008.

Clark, V. R., J. E. Burrows, B. C. Turpin, K. Balkwill, M. Lötter, and S. J. Siebert. 2022. The Limpopo–Mpumalanga–Eswatini Escarpment—Extra-ordinary endemic plant richness and extinction risk in a summer rainfall montane region of Southern Africa. *Frontiers in Ecology and Evolution* 10: 765854.

Cowling, R. M., P. L. Bradshaw, J. F. Colville, and F. Forest. 2017. Levyns' Law: explaining the evolution of a remarkable longitudinal gradient in Cape plant diversity. *Transactions of the Royal Society of South Africa* 72: 184–201.

Cox, F., K. K. Newsham, and C. H. Robinson. 2019. Endemic and cosmopolitan fungal taxa exhibit differential abundances in total and active communities of Antarctic soils. *Environmental Microbiology* 21: 1586–1596.

Crous, P. W., I. H. Rong, A. Wood, S. Lee, H. Glen, W. Botha, B. Slippers, et al. 2006. How many species of fungi are there at the tip of Africa? *Studies in Mycology* 55: 13–33.

Csardi, G., and T. Nepusz. 2006. The igraph software package for complex network research. *InterJournal*, Complex Systems, 1695. Website: https://igraph.org

Culberson, C. F. 1972. Improved conditions and new data for the identification of lichen products by a standardized thin-layer chromatographic method. *Journal of Chromatography* 72: 113–125.

Culberson, C. F., and A. Johnson. 1982. Substitution of methyl *tert*-butyl ether for diethyl ether in the standardized thin-layer chromatographic method for lichen products. *Journal of Chromatography* 128: 253–259.

Culberson, C. F., and H. Kristinsson. 1970. A standardized method for the identification of lichen products. *Journal of Chromatography* 46: 85–93.

Dal Grande, F., G. Rolshausen, P. K. Divakar, A. Crespo, J. Otte, M. Schleuning, and I. Schmitt. 2018. Environment and host identity structure communities of green algal symbionts in lichens. *New Phytologist* 217: 277–289.

De Carolis, R., A. Cometto, P. Moya, E. Barreno, M. Grube, M. Tretiach, S. D. Leavitt, and L. Muggia. 2022. Photobiont diversity in lichen symbioses from extreme environments. *Frontiers in Microbiology* 13: 809804.

De Wever, A., F. Leliaert, E. Verleyen, P. Vanormelingen, K. Van der Gucht, D. A. Hodgson, K. Sabbe, and W. Vyverman. 2009. Hidden levels of phylodiversity in Antarctic green algae: further evidence for the existence of glacial refugia. *Proceedings of the Royal Society, B, Biological Sciences* 276: 3591–3599.

Díaz-Escandón, D., G. Tagirdzhanova, D. Vanderpool, C. C. Allen, A. Aptroot, O. Češka, D. L. Hawksworth, et al. 2022. Genome-level analyses resolve an ancient lineage of symbiotic ascomycetes. *Current Biology* 32: 5209–5218.

Dormann, C. F., J. Fruend, N. Bluethgen, and B. Gruber. 2009. Indices, graphs and null models: analyzing bipartite ecological networks. *Open Ecology Journal* 2: 7–24.

Eichenberger, C., A. Aptroot, and R. Honegger. 2007. Three new *Xanthoria* species from South Africa: *X. hirsuta*, *X. inflata* and *X. doidgeae*. *Lichenologist* 39: 451–458.

Fick, S. E., and R. J. Hijmans. 2017. WorldClim 2: new 1-km spatial resolution climate surfaces for global land areas. *International Journal of Climatology* 37: 4302–4315.

Flechtner, V. R., N. Pietrasiak, and L. A. Lewis. 2013. Newly revealed diversity of green microalgae from wilderness areas of Joshua Tree National Park (JTNP). *Monographs of the Western North American Naturalist* 6: 43–63.

Flessa, F., A. Kehl, M. Imtiaz, and M. Kohl. 2022. *RFLPtools: Tools to analyse RFLP data*. R package version 2.0. Website: https://r-forge.r-project.org/projects/rflptools/

Friedl, T. 1989. Systematik und Biologie von *Trebouxia* (Microthamniales, Chlorophyta) als Phycobiont der Parmeliaceae (lichenisierte Ascomyceten). Ph.D. dissertation, Universitat Bayreuth, Bayreuth, Germany.

Fryday, A. M. 2015. A new checklist of lichenised, lichenicolous and allied fungi reported from South Africa. *Bothalia* 45: 148.

Fryday, A. M., I. D. Medeiros, S. J. Siebert, N. Pope, and N. Rajakaruna. 2020. *Burrowsia*, a new genus of lichenized fungi (Caliciaceae), plus the new species *B. cataractae* and *Scoliciosporum fabisporum*, from Mpumalanga, South Africa. *South African Journal of Botany* 132: 471–481.

Fučíková, K., P. O. Lewis, and L. A. Lewis. 2014. Widespread desert affiliation of trebouxiophycean algae (Trebouxiophyceae, Chlorophyta) including discovery of three new desert genera. *Phycological Research* 62: 294–305.

Gardes, M., and T. D. Bruns. 1993. ITS primers with enhanced specificity for basidiomycetes—application to the identification of mycorrhizae and rusts. *Molecular Ecology* 2: 113–118.

Garrido-Benavent, I., S. Chiva, C. D. Bordenave, A. Molins, and E. Barreno. 2022. *Trebouxia maresiae* sp. nov. (Trebouxiophyceae, Chlorophyta), a new lichenized species of microalga found in coastal environments. *Cryptogamie, Algologie* 43: 135–145.

Garrido-Benavent, I., M. R. Mora-Rodríguez, S. Chiva, S. Fos, and E. Barreno. 2023. *Punctelia borreri* and *P. subrudecta* (Parmeliaceae) associate with a partially overlapping pool of *Trebouxia gelatinosa* lineages. *Lichenologist* 55: 389–399.

Garrido-Benavent, I., S. Pérez-Ortega, A. de los Ríos, and F. Fernández-Mendoza. 2020. Amphitropical variation of the algal partners of *Pseudephebe* (Parmeliaceae, lichenized fungi). *Symbiosis* 82: 35–48.

Gasulla, F., A. Guéra, and E. Barreno. 2010. A simple and rapid method for isolating lichen photobionts. *Symbiosis* 51: 175–179.

Gibbs Russell, G. E. 1987. Preliminary floristic analysis of the major biomes in southern Africa. *Bothalia* 17: 213–227.

Goldblatt, P. 1978. An analysis of the flora of southern Africa: its characteristics, relationships, and origins. *Annals of the Missouri Botanical Garden* 65: 369–436.

González, A. M. M., B. Dalsgaard, and J. M. Olesen. 2010. Centrality measures and the importance of generalist species in pollination networks. *Ecological Complexity* 7: 36–43.

Hale, M. E. 1989. A monograph of the lichen genus *Karoowia* Hale (Ascomycotina: Parmeliaceae). *Mycotaxon* 35: 177–198.

Hale, M. E. 1990. A synopsis of the lichen genus *Xanthoparmelia* (Vainio) Hale (Ascomycotina, Parmeliaceae). *Smithsonian Contributions to Botany* 74: 1–250.

Helms, G. 2003. Taxonomy and symbiosis in associations of Physciaceae and *Trebouxia*. Ph.D. dissertation, Georg-August Universität Göttingen, Göttingen, Germany.

Hestmark, G., F. Lutzoni, and J. Miadlikowska. 2016. Photobiont associations in co-occurring umbilicate lichens with contrasting modes of reproduction in coastal Norway. *Lichenologist* 48: 545–557.

Hijmans, R. 2024. Terra: Spatial data analysis. R package version 1.7-78. Website: https://rspatial.github.io/terra/, https://rspatial.org/

Hilton-Taylor, C. 1996. Patterns and characteristics of the flora of the Succulent Karoo Biome, southern Africa. *In* The biodiversity of African plants: Proceedings XIVth AETFAT Congress, 1994, Wageningen, Netherlands, 58–72. Springer, Dordrecht, Netherlands.

Hoang, D. T., O. Chernomor, A. Von Haeseler, B. Q. Minh, and L. S. Vinh. 2018. UFBoot2: improving the ultrafast bootstrap approximation. *Molecular Biology and Evolution* 35: 518–522.

Hoveka, L. N., M. van Der Bank, B. S. Bezeng, and T. J. Davies. 2020. Identifying biodiversity knowledge gaps for conserving South Africa's endemic flora. *Biodiversity and Conservation* 29: 2803–2819.

Hughes, K.W., A. Case, P. B. Matheny, S. Kivlin, R. H. Petersen, A. N. Miller, and T. Iturriaga. 2020. Secret lifestyles of pyrophilous fungi in the genus *Sphaerosporella*. *American Journal of Botany* 107: 876–885.

Kalyaanamoorthy, S., B. Q. Minh, T. K. Wong, A. Von Haeseler, and L. S. Jermiin. 2017. ModelFinder: fast model selection for accurate phylogenetic estimates. *Nature Methods* 14: 587–589.

Kärnefelt, I., S. Kondratyuk, U. Søchting, and P. Frödén. 2002. *Xanthoria karrooensis* and *X. alexanderbaai* (Teloschistaceae), two new lichen species from southern Africa. *Lichenologist* 34: 333–346.

Katoh, K., J. Rozewicki, and K. D. Yamada. 2019. MAFFT online service: multiple sequence alignment, interactive sequence choice and visualization. *Briefings in Bioinformatics* 20: 1160–1166.

Koch, N. M., J. C. Lendemer, E. A. Manzitto-Tripp, C. McCain, and D. E. Stanton. 2023. Carbon-concentrating mechanisms are a key trait in lichen ecology and distribution. *Ecology* 104: e4011.

Kosecka, M., M. Kukwa, A. Jabłońska, A. Flakus, P. Rodriguez-Flakus, Ł. Ptach, and B. Guzow-Krzemińska. 2022. Phylogeny and ecology of *Trebouxia* photobionts from Bolivian lichens. *Frontiers in Microbiology* 13: 779784.

Kroken, S., and J. W. Taylor. 2000. Phylogenetic species, reproductive mode, and specificity of the green alga *Trebouxia* forming lichens with the fungal genus *Letharia*. *Bryologist* 103: 645–660.

Lange, O.L., E. Kilian, and H. Ziegler. 1986. Water vapor uptake and photosynthesis of lichens: performance differences in species with green and blue-green algae as photobionts. *Oecologia* 71: 104–110.

Lange, O. L., A. Meyer, H. Zellner, and U. Heber. 1994. Photosynthesis and water relations of lichen soil crusts: field measurements in the coastal fog zone of the Namib Desert. *Functional Ecology* 8: 253–264.

Lawrey, J. D. 1980. Sexual and asexual reproductive patterns in *Parmotrema* (Parmeliaceae) that correlate with latitude. *Bryologist* 83: 344–350.

Leavitt, S. D., E. Kraichak, M. P. Nelsen, S. Altermann, P. K. Divakar, D. Alors, T. L. Esslinger, et al. 2015. Fungal specificity and selectivity for algae play a major role in determining lichen partnerships across diverse ecogeographic regions in the lichen-forming family Parmeliaceae (Ascomycota). *Molecular Ecology* 24: 3779–3797.

Leavitt, S. D., P. M. Kirika, G. A. De Paz, J. P. Huang, J.-S. Hur, F. Grewe, P. K. Divakar, and H. T. Lumbsch. 2018. Assessing phylogeny and historical biogeography of the largest genus of lichen-forming fungi, *Xanthoparmelia* (Parmeliaceae, Ascomycota). *Lichenologist* 50: 299–312.

Lewis, L. A., and P. O. Lewis. 2005. Unearthing the molecular phylodiversity of desert soil green algae (Chlorophyta). *Systematic Biology* 54: 936–947.

Lopez, L. C. S., M. P. de Aguiar Fracasso, D. O. Mesquita, A. R. T. Palma, and P. Riul. 2012. The relationship between percentage of singletons and sampling effort: a new approach to reduce the bias of richness estimates. *Ecological Indicators* 14: 164–169.

Lutsak, T., F. Fernández-Mendoza, P. Kirika, M. Wondafrash, and C. Printzen. 2016. Mycobiont–photobiont interactions of the lichen *Cetraria aculeata* in high alpine regions of East Africa and South America. *Symbiosis* 68: 25–37.

Maddison, W. P., and D. R. Maddison. 2021. Mesquite: a modular system for evolutionary analysis, version 3.70. Website: http://www.mesquiteproject.org

Magain, N., J. Miadlikowska, B. Goffinet, E. Sérusiaux, and F. Lutzoni. 2017. Macroevolution of specificity in cyanolichens of the genus *Peltigera* section *Polydactylon* (Lecanoromycetes, Ascomycota). *Systematic Biology* 66: 74–99.

Magain, N., C. Truong, T. Goward, D. Niu, B. Goffinet, E. Sérusiaux, O. Vitikainen, et al. 2018. Species delimitation at a global scale reveals high species richness with complex biogeography and patterns of symbiont association in *Peltigera* section *Peltigera* (lichenized Ascomycota: Lecanoromycetes). *Taxon* 67: 836–870.

Maggs, G. L., P. Craven, and H. H. Kolberg. 1998. Plant species richness, endemism, and genetic resources in Namibia. *Biodiversity & Conservation* 7: 435–446.

Malavasi, V., P. Škaloud, F. Rindi, S. Tempesta, M. Paoletti, and M. Pasqualetti. 2016. DNA-based taxonomy in ecologically versatile microalgae: a re-evaluation of the species concept within the coccoid green algal genus *Coccomyxa* (Trebouxiophyceae, Chlorophyta). *PLoS One* 11: e0151137.

Maphangwa, K. W., C. F. Musil, L. Raitt, and L. Zedda. 2012. Experimental climate warming decreases photosynthetic efficiency of lichens in an arid South African ecosystem. *Oecologia* 169: 257–268.

Marini, L., J. Nascimbene, and P. L. Nimis. 2011. Large-scale patterns of epiphytic lichen species richness: photobiont-dependent response to

climate and forest structure. *Science of the Total Environment* 409: 4381–4386.

Matzer, M., H. Mayrhofer, and G. Rambold. 1997. *Diploicia africana* comb. nov. (lichenized Ascomycetes, Physciaceae), an endemic species from the Cape Province (South Africa). *Nordic Journal of Botany* 17: 433–438.

Medeiros, I. D., and F. Lutzoni. 2022. Contribution to a modern treatment of Graphidaceae biodiversity in South Africa: genera of tribe Graphideae with hyaline ascospores. *Lichenologist* 54: 253–270.

Medeiros, I. D., E. Mazur, J. Miadlikowska, A. Flakus, P. Rodriguez-Flakus, C. J. Pardo-De la Hoz, E. Cieślak, et al. 2021. Turnover of lecanoroid mycobionts and their *Trebouxia* photobionts along an elevation gradient in Bolivia highlights the role of environment in structuring the lichen symbiosis. *Frontiers in Microbiology* 12: 774839.

Meigs, P. 1953. World distribution of arid and semi-arid homoclimates. *In* UNESCO [ed.], Reviews of research on arid zone hydrology, 203–210. UNESCO, Paris, France.

Meyer, C. P., and G. Paulay. 2005. DNA barcoding: error rates based on comprehensive sampling. *PLoS Biology* 3: e422.

Miadlikowska, J., F. Kauff, V. Hofstetter, E. Fraker, M. Grube, J. Hafellner, V. Reeb, et al. 2006. New insights into classification and evolution of the Lecanoromycetes (Pezizomycotina, Ascomycota) from phylogenetic analyses of three ribosomal RNA-and two protein-coding genes. *Mycologia* 98: 1088–1103.

Miller, M. A., W. Pfeiffer, and T. Schwartz. 2010. Creating the CIPRES science gateway for inference of large phylogenetic trees. *In* Proceedings of the Gateway Computing Environments Workshop (GCE), 2010, New Orleans, LA, USA, 1–8. https://doi.org/10.1109/GCE.2010.5676129

Moberg, R. 2004. Notes on foliose species of the lichen family Physciaceae in southern Africa. *Symbolae Botanicae Upsalienses* 34: 257–288.

Molins, A., P. Moya, F. J. García-Breijo, J. Reig-Armiñana, and E. Barreno. 2018. Molecular and morphological diversity of *Trebouxia* microalgae in sphaerothallioid *Circinaria* spp. lichens. *Journal of Phycology* 54: 494–504.

Moya, P., A. Molins, P. Škaloud, P. K. Divakar, S. Chiva, C. Dumitru, M. C. Molina, et al. 2021. Biodiversity patterns and ecological preferences of the photobionts associated with the lichen-forming genus *Parmelia*. *Frontiers in Microbiology* 12: 765310.

Mucina, L., and M. C. Rutherford [eds.]. 2006. The vegetation of South Africa, Lesotho and Swaziland. Strelitzia 19. South African National Biodiversity Institute, Pretoria, South Africa.

Muggia, L., S. D. Leavitt, and E. Barreno. 2018. The hidden diversity of lichenised Trebouxiophyceae (Chlorophyta). *Phycologia* 57: 503–524.

Muggia, L., M. P. Nelsen, P. M. Kirika, E. Barreno, A. Beck, H. Lindgren, H. T. Lumbsch, et al. 2020. Formally described species woefully underrepresent phylogenetic diversity in the common lichen photobiont genus *Trebouxia* (Trebouxiophyceae, Chlorophyta): an impetus for developing an integrated taxonomy. *Molecular Phylogenetics and Evolution* 149: 106821.

Muggia, L., S. Pérez-Ortega, T. Kopun, G. Zellnig, and M. Grube. 2014. Photobiont selectivity leads to ecological tolerance and evolutionary divergence in a polymorphic complex of lichenized fungi. *Annals of Botany* 114: 463–475.

Nelsen, M. P., S. D. Leavitt, K. Heller, L. Muggia, and H. T. Lumbsch. 2021. Macroecological diversification and convergence in a clade of keystone symbionts. *FEMS Microbiology Ecology* 97: fiab072.

Nelsen, M. P., E. Rivas Plata, C. J. Andrew, R. Lücking, and H. T. Lumbsch. 2011. Phylogenetic diversity of Trentepohlialean algae associated with lichen-forming fungi. *Journal of Phycology* 47: 282–290.

Nguyen, L. T., H. A. Schmidt, A. Von Haeseler, and B. Q. Minh. 2015. IQ-TREE: a fast and effective stochastic algorithm for estimating maximum-likelihood phylogenies. *Molecular Biology and Evolution* 32: 268–274.

Nyati, S., D. Bhattacharya, S. Werth, and R. Honegger. 2013. Phylogenetic analysis of LSU and SSU rDNA group I introns of lichen photobionts associated with the genera *Xanthoria* and *Xanthomendoza* (Teloschistaceae, lichenized Ascomycetes). *Journal of Phycology* 49: 1154–1166.

Nyati, S., S. Scherrer, S. Werth, and R. Honegger. 2014. Green-algal photobiont diversity (*Trebouxia* spp.) in representatives of Teloschistaceae (Lecanoromycetes, lichen-forming ascomycetes). *Lichenologist* 46: 189–212.

O'Brien, H. E., J. Miadlikowska, and F. Lutzoni. 2013. Assessing population structure and host specialization in lichenized cyanobacteria. *New Phytologist* 198: 557–566.

Ohmura, Y., M. Kawachi, F. Kasai, M. M. Watanabe, and S. Takeshita. 2006. Genetic combinations of symbionts in a vegetatively reproducing lichen, *Parmotrema tinctorum*, based on ITS rDNA sequences. *Bryologist* 109: 43–59.

Ohmura, Y., S. Takeshita, and M. Kawachi. 2019. Photobiont diversity within populations of a vegetatively reproducing lichen, *Parmotrema tinctorum*, can be generated by photobiont switching. *Symbiosis* 77: 59–72.

Oksanen, J., G. L. Simpson, F. G. Blanchet, R. Kindt, P. Legendre, P. R. Minchin, R. O'Hara, et al. 2022. vegan: Community ecology package, version 2.6-4. Website: https://CRAN.R-project.org/package=vegan

Paul, F., J. Otte, I. Schmitt, and F. Dal Grande. 2018. Comparing Sanger sequencing and high-throughput metabarcoding for inferring photobiont diversity in lichens. *Scientific Reports* 8: 8624.

Paradis, E., and K. Schliep. 2019. ape 5.0: an environment for modern phylogenetics and evolutionary analyses in R. *Bioinformatics* 35: 526–528.

Pedersen, T. 2022. ggraph: An implementation of grammar of graphics for graphs and networks. Websites: https://ggraph.data-imaginist.com, https://github.com/thomasp85/ggraph

Peksa, O., and P. Škaloud. 2011. Do photobionts influence the ecology of lichens? A case study of environmental preferences in symbiotic green alga *Asterochloris* (Trebouxiophyceae). *Molecular Ecology* 20: 3936–3948.

Peksa, O., T. Gebouská, Z. Škvorová, L. Vančurová, and P. Škaloud. 2022. The guilds in green algal lichens—An insight into the life of terrestrial symbiotic communities. *FEMS Microbiology Ecology* 98: fiac008.

Pérez-Ortega, S., M. Verdú, I. Garrido-Benavent, S. Rabasa, T. A. Green, L. G. Sancho, and A. de los Ríos. 2023. Invariant properties of mycobiont-photobiont networks in Antarctic lichens. *Global Ecology and Biogeography* 32: 2033–2046.

Pessi, I. S., Y. Lara, B. Durieu, P. D. C. Maalouf, E. Verleyen, and A. Wilmotte. 2018. Community structure and distribution of benthic cyanobacteria in Antarctic lacustrine microbial mats. *FEMS Microbiology Ecology* 94: fiy042.

Puillandre, N., S. Brouillet, and G. Achaz. 2021. ASAP: assemble species by automatic partitioning. *Molecular Ecology Resources* 21: 609–620.

Puillandre, N., A. Lambert, S. Brouillet, and G. Achaz. 2012. ABGD, Automatic Barcode Gap Discovery for primary species delimitation. *Molecular Ecology* 21: 1864–1877.

de Puymaly, A. 1924. Le *Chlorococcum humicola* (Nag.) Rabenh. *Revue Algologique* 1: 107–114.

R Core Team. 2023. R: a language and environment for statistical computing. R Foundation for Statistical Computing, Vienna, Austria. Website: https://www.R-project.org/

Rafat, A., H. J. Ridgway, R. H. Cruickshank, and H. L. Buckley. 2015. Isolation and co-culturing of symbionts in the genus *Usnea*. *Symbiosis* 66: 123–132.

Rolshausen, G., F. Dal Grande, A. D. Sadowska-Deś, J. Otte, and I. Schmitt. 2018. Quantifying the climatic niche of symbiont partners in a lichen symbiosis indicates mutualist-mediated niche expansions. *Ecography* 41: 1380–1392.

Rolshausen, G., U. Hallman, F. Dal Grande, J. Otte, K. Knudsen, and I. Schmitt. 2020. Expanding the mutualistic niche: parallel symbiont turnover along climatic gradients. *Proceedings of the Royal Society, B, Biological Sciences* 287: 20192311.

Rognes, T., T. Flouri, B. Nichols, C. Quince, and F. Mahé. 2016. VSEARCH: a versatile open source tool for metagenomics. *PeerJ* 4: e2584.

Ruprecht, U., F. Fernández-Mendoza, R. Türk, and A. M. Fryday. 2020. High levels of endemism and local differentiation in the fungal and algal symbionts of saxicolous lecideoid lichens along a latitudinal gradient in southern South America. *Lichenologist* 52: 287–303.

Ryšánek, D., K. Hrčková, and P. Škaloud. 2015. Global ubiquity and local endemism of free-living terrestrial protists: phylogeographic assessment of the streptophyte alga *Klebsormidium*. *Environmental Microbiology* 17: 689–698.

Sadowska-Deś, A. D., M. Bálint, J. Otte, and I. Schmitt. 2013. Assessing intraspecific diversity in a lichen-forming fungus and its green algal symbiont: evaluation of eight molecular markers. *Fungal Ecology* 6: 141–151.

Sadowska-Deś, A. D., F. Dal Grande, H. T. Lumbsch, A. Beck, J. Otte, J.-S. Hur, J. A. Kim, and I. Schmitt. 2014. Integrating coalescent and phylogenetic approaches to delimit species in the lichen photobiont *Trebouxia*. *Molecular Phylogenetics and Evolution* 76: 202–210.

Sanders, W. B., and H. Masumoto. 2021. Lichen algae: the photosynthetic partners in lichen symbioses. *Lichenologist* 53: 347–393.

Schieferstein, B., and K. Loris. 1992. Ecological investigations on lichen fields of the Central Namib: I. Distribution patterns and habitat conditions. *Vegetatio* 98: 113–128.

Schloss, P. D., S. L. Westcott, T. Ryabin, J. R. Hall, M. Hartmann, E. B. Hollister, R. A. Lesniewski, et al. 2009. Introducing mothur: open-source, platform-independent, community-supported software for describing and comparing microbial communities. *Applied and Environmental Microbiology* 75: 7537–7541.

Schnitzler, J., T. G. Barraclough, J. S. Boatwright, P. Goldblatt, J. C. Manning, M. P. Powell, T. Rebelo, and V. Savolainen. 2011. Causes of plant diversification in the Cape biodiversity hotspot of South Africa. *Systematic Biology* 60: 343–357.

Simmons, R. E., M. Griffin, R. E. Griffin, E. Marais, and H. Kolberg. 1998. Endemism in Namibia: patterns, processes and predictions. *Biodiversity & Conservation* 7: 513–530.

Sipman, H. 2017. Compiled key to *Xanthoparmelia* in Southern Africa. Website: https://archive.bgbm.org/BGBM/STAFF/Wiss/Sipman/keys/Afroxantkey3a.pdf [accessed 3 August 2023].

Singh, G., F. Dal Grande, P. K. Divakar, J. Otte, A. Crespo, and I. Schmitt. 2017. Fungal–algal association patterns in lichen symbiosis linked to macroclimate. *New Phytologist* 214: 317–329.

Škaloud, P., J. Steinová, T. Řídká, L. Vančurová, and O. Peksa. 2015. Assembling the challenging puzzle of algal biodiversity: species delimitation within the genus *Asterochloris* (Trebouxiophyceae, Chlorophyta). *Journal of Phycology* 51: 507–527.

Škaloud, P., P. Moya, A. Molins, O. Peksa, A. Santos-Guerra, and E. Barreno. 2018. Untangling the hidden intrathalline microalgal diversity in *Parmotrema pseudotinctorum*: *Trebouxia crespoana* sp. nov. *Lichenologist* 50: 357–369.

Stevens, G. N. 1999. A revision of the lichen family Usneaceae in Australia. *Bibliotheca Lichenologica* 72: 1–128.

Swinscow, T. D. V., and H. Krog. 1988. Macrolichens of East Africa. British Museum (Natural History), London, UK.

Vančurová, L., J. Malíček, J. Steinová, and P. Škaloud. 2021. Choosing the right life partner: Ecological drivers of lichen symbiosis. *Frontiers in Microbiology* 12: 769304.

Vančurová, L., L. Muggia, O. Peksa, T. Řídká, and P. Škaloud. 2018. The complexity of symbiotic interactions influences the ecological amplitude of the host: a case study in *Stereocaulon* (lichenized Ascomycota). *Molecular Ecology* 27: 3016–3033.

van der Niet, T., and S. D. Johnson. 2009. Patterns of plant speciation in the Cape floristic region. *Molecular Phylogenetics and Evolution* 51: 85–93.

Vargas Castillo, R., and A. Beck. 2012. Photobiont selectivity and specificity in *Caloplaca* species in a fog-induced community in the Atacama Desert, northern Chile. *Fungal Biology* 116: 665–676.

Vázquez, D. P., C. J. Melian, N. M. Williams, N. Blüthgen, B. R. Krasnov, and R. Poulin. 2007. Species abundance and asymmetric interaction strength in ecological networks. *Oikos* 116: 1120–1127.

Verboom, G. A., J. K. Archibald, F. T. Bakker, D. U. Bellstedt, F. Conrad, L. L. Dreyer, F. Forest, et al. 2009. Origin and diversification of the Greater Cape flora: ancient species repository, hot-bed of recent radiation, or both? *Molecular Phylogenetics and Evolution* 51: 44–53.

Vilgalys, R., and M. Hester. 1990. Rapid genetic identification and mapping of enzymatically amplified ribosomal DNA from several *Cryptococcus* species. *Journal of Bacteriology* 172: 4238–4246.

Wagner, M., G. Brunauer, A. C. Bathke, S. C. Cary, R. Fuchs, L. G. Sancho, R. Türk, and U. Ruprecht. 2021. Macroclimatic conditions as main drivers for symbiotic association patterns in lecideoid lichens along the Transantarctic Mountains, Ross Sea region, Antarctica. *Scientific Reports* 11: 23460.

Werth, S., and V. L. Sork. 2010. Identity and genetic structure of the photobiont of the epiphytic lichen *Ramalina menziesii* on three oak species in southern California. *American Journal of Botany* 97: 821–830.

Wessels, D., and L. Kappen. 1993. Photosynthetic performance of rock-colonising lichens in the Mountain Zebra National Park, South Africa. *Koedoe* 36: 27–48.

White, T. J., T. Bruns, S. Lee, and J. Taylor. 1990. Amplification and direct sequencing of fungal ribosomal RNA genes for phylogenetics. *In* M. A. Innis, D. H. Gelfand, J. J. Sninsky, and T. J. White [eds.], PCR protocols: a guide to methods and applications, 315–322. Academic Press, London, UK.

Whittaker, R. H. 1960. Vegetation of the Siskiyou mountains, Oregon and California. *Ecological Monographs* 30: 279–338.

Wiemers, M., and K. Fiedler. 2007. Does the DNA barcoding gap exist? A case study in blue butterflies (Lepidoptera: Lycaenidae). *Frontiers in Zoology* 4: 8.

Wirth, V. 2010. Lichens of the Namib Desert: a guide to their identification. Klaus Hess, Göttingen, Germany.

Wolseley, P. 1997. Response of epiphytic lichens to fire in tropical forests of Thailand. *Bibliotheca Lichenologica* 68: 165–176.

Xu, M., H. De Boer, E. S. Olafsdottir, S. Omarsdottir, and S. Heidmarsson. 2020. Phylogenetic diversity of the lichenized algal genus *Trebouxia* (Trebouxiophyceae, Chlorophyta): a new lineage and novel insights from fungal-algal association patterns of Icelandic cetrarioid lichens (Parmeliaceae, Ascomycota). *Botanical Journal of the Linnean Society* 194: 460–468.

Xu, S., Z. Dai, P. Guo, X. Fu, S. Liu, L. Zhou, W. Tang, et al. 2021. ggtreeExtra: Compact visualization of richly annotated phylogenetic data. *Molecular Biology and Evolution* 38: 4039–4042.

Yu, G., D. K. Smith, H. Zhu, Y. Guan, and T. T. Y. Lam. 2017. ggtree: an R package for visualization and annotation of phylogenetic trees with their covariates and other associated data. *Methods in Ecology and Evolution* 8: 28–36.

Zedda, L., and G. Rambold. 2009. Diversity and ecology of soil lichens in the Knersvlakte (South Africa). *Bryologist* 112: 19–29.

Zhang, J., P. Kapli, P. Pavlidis, and A. Stamatakis. 2013. A general species delimitation method with applications to phylogenetic placements. *Bioinformatics* 29: 2869–2876.

Zhang, Z., S. Schwartz, L. Wagner, and W. Miller. 2000. A greedy algorithm for aligning DNA sequences. *Journal of Computational Biology* 7: 203–214.

Zoller, S., C. Scheidegger, and C. Sperisen. 1999. PCR primers for the amplification of mitochondrial small subunit ribosomal DNA of lichen-forming ascomycetes. *Lichenologist* 31: 511–516.

## SUPPORTING INFORMATION

Additional supporting information can be found online in the Supporting Information section at the end of this article.

**Appendix S1**. Previously available molecular data for lichen photobionts of South Africa.

**Appendix S2**. Infrageneric phylogenetic classification of *Trebouxia* and summary of data available on GenBank.

**Appendix S3**. Protected areas in southern Africa sampled for lichenized *Trebouxia*.

**Appendix S4**. Table of voucher and GenBank accession data for southern African *Trebouxia* sequences generated in this study or downloaded from GenBank.

**Appendix S5**. Table of voucher and GenBank accession data for sequences of green algal photobionts other than *Trebouxia* generated in this study.

**Appendix S6**. Table of sample names and GenBank accessions for non-southern African nrITS and *rbcL* sequences used in the data set A phylogenetic analyses.

**Appendix S7**. Statistics on the data set A alignments for southern African *Trebouxia*.

**Appendix S8**. Table of GenBank accessions excluded from data set B (OTU clustering and barcode gap analyses) with justifications for each exclusion.

**Appendix S9**. Concatenated nrITS-*rbcL* maximum likelihood phylogenies of *Trebouxia* clades A, C, I, and S (dataset A) displaying ultrafast bootstrap values ≥ 50.

**Appendix S10**. Table of nrITS GenBank accessions included in data set B, with corresponding 95% and 97% clusters and classification in the framework of Muggia et al. (2020).

**Appendix S11**. Sankey diagram comparing the 95% OTU clustering, monophyly-known species, 97% OTU clustering, and maximum likelihood implementation of PTP (PTP-ML) approaches to classifying southern African *Trebouxia*.

**Appendix S12**. Estimates of global species richness in *Trebouxia*.

**Appendix S13**. Analyses based on 97% OTU clustering: Species accumulation curve for southern African *Trebouxia* and comparison to *Trebouxia* biota of Kenya and Bolivia.

**Appendix S14**. Histograms showing results of randomization tests (i.e., null distributions) for an association between the GCFR or desert and novel, putative endemic *Trebouxia* species.

**Appendix S15**. Maps showing the number of *Trebouxia* species in each major clade sampled from the sites in Figure 1.

**Appendix S16**. Robustness checks for the site–photobiont network.

**Appendix S17**. Site–photobiont and mycobiont–photobiont network based on the 97% OTU clustering *Trebouxia* species delimitation.

**Appendix S18**. Results for modularity, photobiont nestedness, and mycobiont nestedness in the mycobiont genus–photobiont species network under the *Trebouxia* consensus classification.

**Appendix S19**. Top five most important mycobionts and photobionts for the connectivity of the *Trebouxia* species–mycobiont genus network, ranked by betweenness centrality.

**Appendix S20**. Classification of putative *Trebouxia* species introduced by Ruprecht et al. (2020) using alphanumeric codes overlapping with new species delimited by Muggia et al. (2020).

**How to cite this article:** Medeiros, I. D., A. Ibáñez, A. E. Arnold, T. A. Hedderson, J. Miadlikowska, A. Flakus, I. Carbone, et al. 2024. Eco-phylogenetic study of *Trebouxia* in southern Africa reveals interbiome connectivity and potential endemism in a green algal lichen photobiont. *American Journal of Botany* 111(12): e16441. https://doi.org/10.1002/ajb2.16441